University of BRISTOL

Investigating the role of EZH2 in the BASP1/WT1 repressive complex

Marina Johnson

A dissertation submitted to the University of Bristol in accordance with the requirements for award of the degree of MSc by Research in the Faculty of Life Sciences.

School of Cellular and Molecular Medicine

September 2019

Word Count: 12190

Table of Contents

Abstract

BASP1 is a neuronal signalling protein that was found to be a corepressor of the developmental transcription factor Wilms' tumour 1 (WT1). Both BASP1 and WT1 are involved in several different types of cancer and can act as both tumour suppressors and oncogenes. Together, they form the BASP1/WT1 repressive complex which can inhibit the transcription of WT1 target genes. Recent studies in understanding the repressive mechanism of this complex showed that BASP1 facilitates the removal of activatory histone marks (H3K4me^3 and H3K9ac) and the placement of repressive histone marks (H3K9me^3 and H3K27me^3). EZH2, a core subunit of the polycomb (PRC2) complex, was found to be recruited to the promoter region of WT1 target genes by BASP1. EZH2 is a histone methyltransferase which places H3K27me^3 marks on gene promoters. Whether or not EZH2 is the enzyme that places the BASP1-dependent H3K27me^3 mark and is involved in the transcriptional repression mechanism of BASP1 is not known.

This study used three different EZH2 inhibitors to examine the role of EZH2 in BASP1-dependent transcriptional repression in two different cell lines. The work revealed that EZH2 is responsible for placing BASP1-dependent H3K27me^3 marks on the promoters of WT1 target genes. However, the BASP1/WT1 complex exhibited different requirements for EZH2 activity in transcriptional repression depending on the specific target gene.

The effects of EZH2 inhibition on BASP1-dependent suppression of cancer cell growth was also studied. The results showed that, in the absence of EZH2, K562 cells had a decreased growth rate and MCF7 cells showed decreased tumorigenicity, suggesting that the BASP1/WT1 complex works with EZH2 to repress growth-promoting genes.

The findings indicate that the BASP1/WT1 complex employs multiple mechanisms to mediate gene repression. The results suggest that EZH2 plays a role in the function of this complex but the effects on transcriptional repression are gene specific.

Acknowledgements

First, I would like to thank my supervisor Professor Stefan Roberts for his constant guidance and support throughout this project. His valuable feedback and positive attitude helped me achieve the best I could and made the whole process an enjoyable experience.

Second, I would like to thank Dr Amy Dey from Professor Roberts' lab who optimised the ChIP experiment for this study and taught me how to do it. I would also like to thank Dr Keith Brown, who monitored my progress throughout this process and provided valuable insight about my experiments.

I would also like to thank Dr Natasha Clayton, Dr Camilla Cerutti, Victoria Swann and Anna Fleming for the much-needed breaks in the office and venting when our experiments didn't work. They and everyone in the G66 lab made it a great environment to work in.

Finally, I would like to thank my family for always encouraging me to pursue my goals. Their unmeasurable love and support throughout my whole life and especially during this past year have helped me be where I am today.

Declaration

I declare that the work in this dissertation was carried out in accordance with the requirements of the University's *Regulations and Code of Practice for Research Degree Programmes* and that it has not been submitted for any other academic award. Except where indicated by specific reference in the text, the work is the candidate's own work. Work done in collaboration with, or with the assistance of, others, is indicated as such. Any views expressed in the dissertation are those of the author.

SIGNED: ..... DATE: .....

List of Figures

Abbreviations

ALL	Acute Lymphoblastic Leukaemia
AML	Acute Myeloid Leukaemia
BASP1	Brain Acid Soluble Protein 1
CBP	CREB-Binding Protein
ChIP	Chromatin Immunoprecipitation
CLL	Chronic Lymphoblastic Leukaemia
CML	Chronic Myeloid Leukaemia
CRAC	Cholesterol Recognition Amino Acid Consensus
DMSO	Dimethyl Sulfoxide
DNA	Deoxyribonucleic Acid
DTT	Dithiothreitol
EDTA	Ethylene Diamine Tetraacetic Acid
EED	Embryonic Ectoderm Development
EMT	Epithelial Mesenchymal Transition
ERα	Oestrogen Receptor α
ESC	Embryonic Stem Cell
EZH2	Enhancer of Zeste Homologue 2
HAT	Histone Acetyl Transferase
HDAC	Histone Deacetylase
HMT	Histone Methyl Transferase
KCl	Potassium Chloride
kDa	Kilo Dalton
KTS	Lysine, Threonine, Serine
LiCl	Lithium Chloride
$MgCl_2$	Magnesium Chloride
NaCl	Sodium Chloride
NP-40	Nonident P40
PAGE	Polyacrylamide Gel Electrophoresis
PBS	Phosphate Buffered Saline
PcG	Polycomb group
PCL	Polycomb-like
PCR	Polymerase Chain Reaction
PEST	Proline, Glutamic acid, Serine, Threonine
PIP_2	Phosphatidylinositol 4,5-biphosphate
PKA	Protein Kinase A
PKC	Protein Kinase C
PRC2	Polycomb Repressive Complex
RNA	Ribonucleic acid
SAM	S-adenosyl-L-Methionine
SDS	Sodium Dodecyl Sulfate
SUZ12	Suppressor of Zeste 12
TSG	Tumour Suppressor Gene
WT	Wilms Tumour
WT1	Wilms' Tumour 1

1.Introduction

1.1 WT1

One of the first tumour suppressor genes (TSG) to be identified and cloned was the transcription factor Wilms' Tumour 1 (WT1). It was discovered due to its involvement in the paediatric kidney cancer Wilms' Tumour (WT) [1].WT is one of the most common childhood solid cancers, affecting 1 in every 10 000 children[2]. This is because WT1 plays a central role ins regulating kidney development during embryogenesis and was found to be mutated in 15% of WT cases. Interest in WT1 arose when it was found that as a transcription factor it can affect a range of cell processes. WT1 controls the expression of genes that affect cell apoptosis, growth and differentiation[3]. The ability of WT1 to control the expression of genes involved in both cell growth and cell death relies on its ability to act as both an activator and repressor of transcription, depending on the cofactors it interacts with[4].

1.1.1 WT1 Structure, isoforms and function

The WT1 gene is found at the chromosome locus 11p13 and is approximately 50kb[5]. As seen in Figure 1.1, WT1 is made up of four zinc fingers at its C-terminus that allow it to bind to DNA and a proline and glutamine-rich region at its N-terminus [6]. It has a transcriptional repression domain between residues 71-180 and a transcriptional activation domain between residues 180-250 that act independently to allow WT1 to activate or repress a range of target genes[7]. The WT1 gene includes 10 exons that can undergo alternative splicing, use of alternative translation start sites and RNA editing to generate over 24 different isoforms[8]. Two of the most studied isoforms in mammals arise from alternative splicing of exon 9 which leads to either the removal or addition of a three amino acid sequence made up of lysine, threonine and serine (KTS), between zinc fingers 3 and 4 [9]. These two isoforms are highly conserved in all vertebrates. The +KTS isoform of WT1 is known to bind to RNA with higher affinity and has an important role during gonad development [3,10]. The -KTS isoform of WT1 is known to bind to DNA with higher affinity and has an important role in kidney development and podocyte differentiation. Exon 5 of the WT1 gene also commonly undergoes alternative splicing resulting in the addition of a 17 amino acid sequence (+17AA). This WT1 isoform is only found in mammalian cells and its function is not yet known[11]. WT1 can also undergo several

post-translational modifications. It can be SUMOylated at two lysine residues (Lys73 and Lys177) located within the transcriptional repression domain at the N-terminus[12]. The effect of this modification is not yet known however it has been proposed to affect the association of WT1 with its cofactors that are also SUMOylated. WT1 can also be phosphorylated at serine 365 within zinc finger 2 by protein kinase A (PKA) and at serine 393 within zinc finger 3 by protein kinase C (PKC) [13]. These phosphorylation events decrease the ability of WT1 to regulate transcription by preventing it from binding to DNA [14].

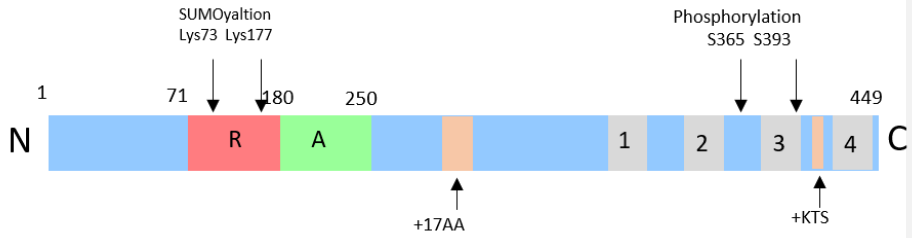

Figure 1.1: A schematic of the primary structure of the WT1 protein. The sites where alternative splicing occurs are shown in orange (+17AA and +KTS). The sites of post-translational modifications are shown as SUMOylation and phosphorylation. The transcriptional repression domain is shown in red (R) and the transcriptional activation domain is shown in green (A). The 4 zinc fingers are found at the C-terminus in grey (1,2,3,4).

Due to the ability of WT1 to act as both a transcriptional repressor and activator, the mechanisms by which it acts as a transcriptional regulator are complex and depend on the cofactors interacting with WT1[4]. CBP is a histone acetyl transferase (HAT) that interacts with WT1 to promote transcriptional activation of target genes[15]. Brain acid soluble protein 1(BASP1) associates with WT1 to promote transcription repression by recruiting histone deacetylases (HDAC)[16]. WT1 can also bind to other DNA-binding proteins such as p53, which allows it to be recruited to target gene promoters[17]. The main way WT1 localises to promoters, however, is by directly binding to the DNA.

The ability of WT1 to act as transcriptional regulator by either activating or repressing genes underlies its fundamental roles during embryogenesis. WT1 is

involved in the normal development of the kidneys, heart, gonads, spleen and many other organs[18]. Several developmental disorders can occur due to mutation of WT1 which emphasises its important functions during development. Denys-Drash syndrome leads to severe developmental abnormalities such as hermaphroditism and renal failure and can be caused by intergenic mutations in exons 8 and 9 of WT1 where the DNA-binding domains are found[19]. Heterozygous deletions of WT1 resulting in loss of WT1 function can result in the development of WT, aniridia, genitourinary abnormalities and mental retardation, also known as WAGR syndrome[20].Developmental abnormalities are not the only disorders associated with WT1. WT1 mutations have also been associated with a number of ~~fr~~ different cancers including lung, prostate, leukaemias and Wilms' tumour.

1.1.2 WT1 in cancer

WT1 was first identified to be involved in cancer in Wilms' Tumour as a TSG. In 10-15% of Wilms' tumours WT1 is inactivated which results in increased cell proliferation and survival[1]. WT1 has since also been found to act as an oncogene in adult cancers where it is expressed in tissues where it is not normally found such as the colon, breast and brain[21–24]. Overexpression of WT1 promotes angiogenesis and vascularisation and in leukaemias such as AML, ALL and CLL, high levels of WT1 are associated with a poor prognosis[25].

1.2 BASP1

BASP1 was originally isolated from brain cells as a member of the neuronal signalling protein family and was later found to be expressed in many other neuronal cell types[26]. It was then found that BASP1 is in fact widely expressed including at sites such as the kidney, spleen and gonads where there are also high levels of WT1 expression. Further studies into the relationship between BASP1 and WT1 found that BASP1 acts a cosuppressor to WT1 by binding to it and so preventing transcription of WT1 target genes[16].

1.1.3 BASP1 Structure and Properties

BASP1 is a highly charged protein that was initially found to be cytoplasmic and membrane localised[26]. Subsequent studies have since shown that BASP1 is also ~~be~~ present in the nucleus. It belongs to a family of neuronal signalling proteins along with GAP43 and MARCKS which are found in high amounts in nerve cells[27] .

These proteins share similar properties like the ability to bind to cell membrane phospholipids, but their primary structures are very different. As seen in Figure 1.2, BASP1 has a membrane binding domain at its N-terminus where a myristoyl group can be added on the α-amino group of the glycine residue at position 2. Myristylation of BASP1 occurs co-translationally and it allows this hydrophilic protein to interact with cell membranes[28]. It also has a basic region which helps BASP1 to interact with acidic phospholipids like phosphatidylinositol 4,5-biphosphate (PIP_2) and Ca^{2+} bound calmodulin. The first N-terminal 18 amino acid sequence of BASP1 contains the glycine on which the myristoyl group is added as well as a cholesterol recognition amino acid consensus (CRAC) domain which allows BASP1 to interact with cholesterol[29]. This region of BASP1 is highly conserved across vertebrates, highlighting the importance of PIP_2 and cholesterol interactions of BASP1[26]. BASP1 has 3 PEST domains indicative of a high turnover protein which are also highly conserved[30]. PKC can phosphorylate BASP1 at multiple serine residues. Phosphorylation at Ser6 can disrupt the positive charge of the N-terminus and results in the destabilisation of BASP1-lipid interactions [28]. Many of the other phosphorylation sites are found within the PEST sequences which suggests that PKC has a role in regulating BASP1 stability. BASP1 can also be sumoylated at specific lysine residues and this causes its redistribution from chromatin to the nuclear matrix[10].

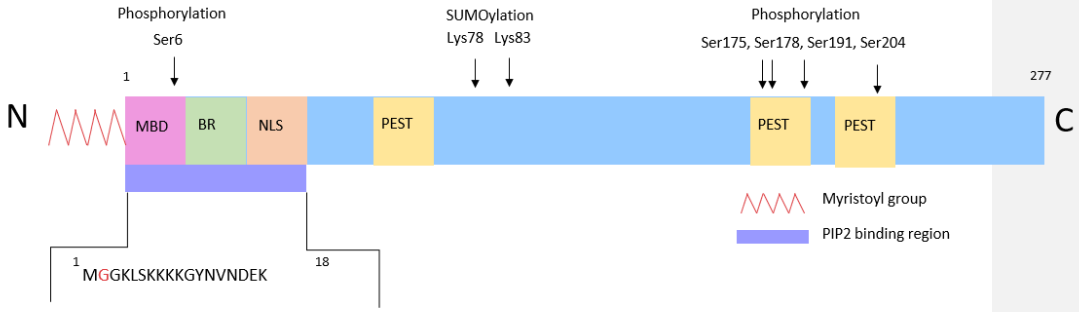

Figure 1.2: The structure of the BASP1 protein. BASP1 contains an N-terminal membrane binding domain (MBD), a basic region (BR) and a nuclear localisation sequence (NLS) at the N-terminus. This region forms the binding site for PIP_2. The N-terminal glycine residue (in red) is myristoylated. The 3 PEST domains are shown in yellow. BASP1 is phosphorylated at the indicated serine residues and sumoylated at the indicated lysine residues.

1.2.2 BASP1 in cancer

BASP1 is involved in many different types of cancer where it frequently acts as a TSG[27] . In thyroid cancer, overexpression of BASP1 decreases cancer cell growth by causing G1 cell cycle arrest via Cyclin D1 inhibition and p21 and p27 activation[31]. Overexpression of BASP1 was also seen to prevent cancer cell migration by inhibiting β-catenin and E-cadherin. This suggests BASP1 has a role as a TSG in thyroid cancer and a poor prognosis has been associated with low levels of BASP1. In hepatocellular carcinomas BASP1 expression is significantly decreased by promoter methylation in the cancer cells compared to normal cells[32]. In breast cancer BASP1 can act as a transcriptional cosuppressor of ERα, which is a hormone receptor involved in regulating proliferation and differentiation genes[33]. This interaction is enhanced by treatment of breast cancer cells with tamoxifen (a drug normally given as part of breast cancer treatment). BASP1 can enhance the growth inhibitory effect of tamoxifen through its interaction with ERα[33][34]. BASP1 was also recently shown to act as an oncogene in cervical cancer where it becomes upregulated leading to increased cell proliferation[34].

1.2.3 BASP1/WT1 in differentiation

With the ability to repress several genes, the BASP1/WT1 complex was also found to be involved in several differentiation pathways by controlling the expression of the genes involved. The BASP1/WT1 complex can change the differentiation pathway of K562 leukaemia cells following PMA treatment[25]. K562 express endogenous WT1 but do not express BASP1 and will normally differentiate into megakaryocytes when treated with PMA. However, K562 cells engineered to express BASP1 will differentiate into elongated neuronal-like cells. This happens because BASP1 can alter the PMA-induced expression profile away from megakaryocyte-associated genes towards genes with neuronal function. The BASP1/WT1 complex is also involved in the differentiation pathway of taste receptor cells. During development of the taste receptor cells only WT1 is expressed but once they begin to differentiate, they start to express BASP1. BASP1 expression is maintained in adult taste buds where it colocalises with WT1 at the promoter regions of target genes. BASP1 expression in mature taste cells is essential for taste detection[35]. BASP1 inhibits the expression of LEF1 of the Wnt pathway and PTCH1 of the Shh pathway, which are both WT1 target genes. The expression of these

genes is normally associated with the progenitor cells and thus their repression by the WT1/BASP1 complex is needed to maintain the differentiation state of taste receptor cells[36,37]. A similar pattern has been observed in stem cells where multipotency is maintained when WT1 is expressed alone and when BASP1 is switched on multipotency is blocked and stem cells are driven to differentiate[38]. These effects of BASP1 were studied using induced pluripotent stem cells (iPSCs) made by transient expression of Oct4, Sox2, Klf4 and c-Myc, also known as the OSKM cocktail[39]. Antibody-mediated inhibition of BASP1 was found to be able to replace the need for Sox2 in the OSKM cocktail, further confirming that the presence of BASP1 inhibits the reprogramming of cells. Further studies found that this was because BASP1 repressed the expression of the WT1 target gene Lin28. Lin28 is an RNA-binding protein that can promote pluripotency by regulating Let-7 miRNA[40]. These results suggest an interesting interplay between BASP1 and WT1 during the development of stem cells and could have potential therapeutic roles.

1.2.4 BASP1/WT1 Repressive Complex

The presence of BASP1 at sites of high WT1 activity suggested that these two proteins work together to ensure normal embryonic development. Genome-wide studies have shown that BASP1 can regulate over 1000 different genes in K562 cells. Moreover, BASP1 regulates the activity of other transcription factors like ERα. However it has mostly been studied as a cosuppressor of WT1 and therefore it is best understood as a part of the BASP1/WT1 repressive complex[25]. In recent years it has been shown that BASP1 can bind to the suppression domain of WT1 and mediate repression of WT1 target genes by recruiting a number of different cofactors at target gene promoters[16]. The recruitment of most cofactors by BASP1 requires the myristoyl group located at its N-terminus which allows BASP1 to interact with PIP_2 and so recruit additional cofactors[28]. A mutant BASP1 derivative where the myristoyl acceptor glycine is replaced with an alanine (BASP1 G2A) cannot act as a transcriptional cosuppressor of WT1. In Figure 1.3 it is shown that the BASP1/WT1 repression complex recruits HDAC1 which removes negatively charged acetyl groups from histone sites like histone 3 lysine 9 (H3K9ac)[28]. It also recruits prohibitin which in turn recruits BRG1 of the ATP-dependent chromatin remodelling SWI/SNF complex which promotes transcriptional repression[41,42].

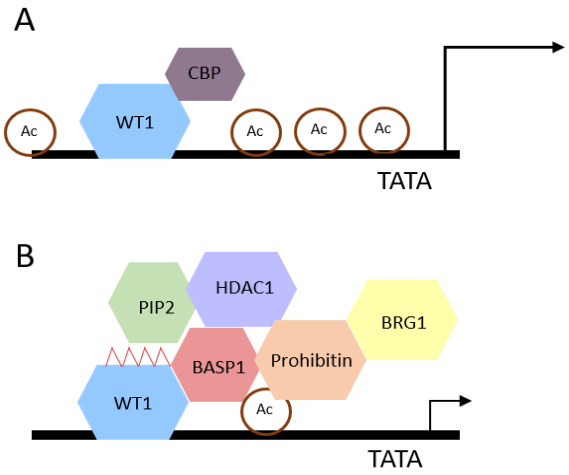

Figure 1.3: Removal of histone acetyl groups by the BASP1/WT1 complex. (A) The WT1-CBP activator complex. WT1 interacts with the histone acetyl transferase CBP to place~~add~~ acetylation marks on gene promoters and activate gene expression. **(B)** the WT1-BASP1 repressor complex. BASP1 binds to WT1 and recruits PIP_2, HDAC1, Prohibitn and BRG1 on gene promoters through its N-terminal myristoyl group to remove acetyl groups and repress gene transcription.

Recent studies using the BASP1 G2A mutant derivative showed that myristoylation of BASP1 is required to deacetylate histone H3K9 at the promoter of WT1 target genes. This action of BASP1 is therefore lipid dependent[43]. It was ~~also~~ shown that BASP1 can also remove methyl groups from lysine 4 of histone 3 ($H3K4me^3$) which are also activatory marks. This action is also lipid dependent. Additional to removing these activation marks, BASP1 can also add repressive marks such as methyl groups on histone 3 lysine 27 ($H3K27me^3$) and on histone 3 lysine 9 ($H3K9me^3$) as can be seen in Figure 1.4[43]. The addition of these repressive marks was found to be supported by the G2A mutant BASP1, indicating that this action by BASP1 is lipid independent.

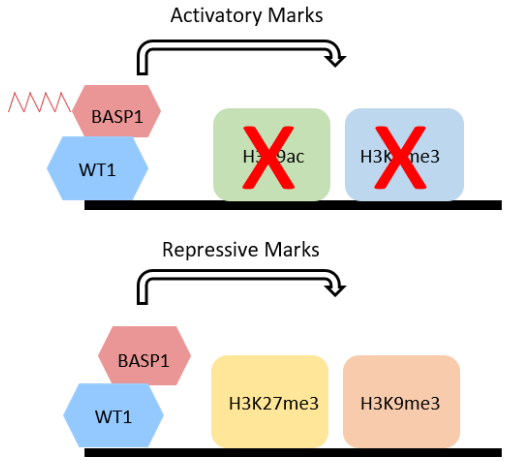

Figure 1.4: The BASP1/WT1 complex effect on histone chromatin marks. The WT1-BASP1 complex can remove activatory marks H3K9ac and H3K4me3 and this process is lipid-dependent because BASP1 needs to be myristoylated. BASP1 can place repressive marks H3K27me3 and H3K9me3 and this process is lipid independent because BASP1 does not need to be myristoylated.

Formatted: Font: Not Bold

1.2.5 BASP1/WT1 lipid independent transcriptional repression

BASP1 was first shown to be involved in the placement of repressive chromatin marks, specifically H3K27me^3 at the Wnt4 locus, during the differentiation of epicardial cells [44]. This locus is regulated by the BASP1/WT1 complex and controls epithelial-mesenchymal transition (EMT) and the generation of progenitor cardiovascular cells[45]. As mentioned above, BASP1 has also been observed to add H3K27me^3 marks as well as H3K9me^3 marks on the promoter regions of WT1 target genes and this action is lipid independent. The addition of repressive marks however is not sufficient to repress transcription of these genes[43]. The BASP1 G2A mutant does not repress transcription of these genes despite being shown to be able to place H3K27me^3 marks. These results demonstrate that the removal of activatory marks is required for transcriptional repression by BASP1. However, it is not yet known if the addition of repressive marks is essential for BASP1 to carry out its role as a cosuppressor of WT1. Sites that have both activatory and repressive marks present are known as bivalent and are associated with embryonic stem cells[46]. The activatory marks are known to be removed by HDAC1 and prohibitin, however it is

unclear how the repressive methylation marks are added. The enhancer of zeste homologue 2 (EZH2) subunit of the Polycomb repressive complex 2 (PRC2) is widely known for placing H3K27me^3 marks as well as H3K9me^3 marks[47]. Further studies using Chromatin Immunoprecipitation (ChIP) experiments showed that EZH2 is in fact recruited to the promoter regions of WT1 target genes in cells expressing BASP1[43]. BASP1-G2A cells can also recruit EZH2 indicating that, like the addition of repressive marks, this process is independent of BASP1 lipidation. These findings suggest that the addition of repressive marks by BASP1 might be mediated by the PRC2 complex.

1.3 EZH2

1.3.1 PRC2 Structure and Function

EZH2 is the main enzymatic subunit of PRC2 that acts as a histone methyltransferase to catalyse the mono-, di- and tri-methylation of H3K27[48]. PRC2 belongs to a family of Polycomb group (PcG) proteins originally identified in Drosophila which are chromatin-associated factors that have an important role in maintaining the transcriptionally silent state of genes during early development[49]. PRC2 is essential during embryonic development as it targets and represses developmental genes in embryonic stem cells (ESCs) to maintain pluripotency[50,51].EZH2 is a core subunit of PRC2 alongside Suppressor of Zest 12 (SUZ12) and embryonic ectoderm development (EED)[52]. EZH2 can be replaced by its homologue EZH1 as the catalytic subunit of PRC2 and in fact EZH2 is only expressed in actively dividing cells whereas EZH1 is ubiquitously expressed making it the most abundant subunit[53–55]. PRC2-EZH1 and PRC2-EZH2 exhibit different levels of histone methyltransferase activity, with PRC2-EZH2 showing higher levels of activity and so PRC2 is able to switch between EZH1 and EZH2 based on the differentiation state of the cell[55,56]. PRC2-EZH2 was found to have a more important role in actively dividing cells whereas PRC2-EZH1 was found to have a more important role in cells completing the differentiation process. The three core subunits are essential for PRC2 activity and if deleted they are embryonic lethal in mice and flies[57]. PRC2 can also interact with other factors to produce different subcomplexes which have been subcategorised in two main subtypes, PRC2.1 and PRC2.2[58]. PRC2 can interact with PCL homologues PCL1-3 and EPOP or PALI to form the PRC2.1 subtype or it can interact with JARID2 and AEBP2 to from the PRC2.2 subtype. Both subtypes also interact with the histone-

binding protein RBBP46/48[59]. It was suggested that the two different PRC2 subunits target different genes but ChIP-seq studies have shown that they have overlapping target sites suggesting that the two subunits work together to recruit the core PRC2 subunits[60–63]. Another member of the PcG proteins is PRC1 which has distinct enzymatic activities to PRC2 and is responsible for catalysing the monoubiquitination of Lysine 119 on histone H2A (H2AK119ub)[64]. PRC1 and PRC2 have been observed to have overlapping genomic binding patterns and so are thought to work together to establish transcriptional repression[65,66].

1.3.2 EZH2 in cancer

Multiple studies have confirmed that EZH2 plays an important role in the development of many cancers[67]. In prostate, breast, bladder and endometrial cancer EZH2 is overexpressed which is associated with a more aggressive progression of the cancer and a poor prognosis[68,69]. In cancer cell lines EZH2 has been shown to be essential for their proliferation and so cancers that ectopically express EZH2 are considered to have a proliferative advantage[70]. Additional to being overexpressed, EZH2 can undergo numerous gain-of-function mutations that can promote tumorigenesis. Point mutations affecting the SET domain of EZH2 result in increased H3K27me^3 and have been identified in 7-12% of follicular lymphomas [71,72]. Similarly, point mutations at EZH2 alanine residues within its catalytic SET domain result in increased H3K27me^3 and have been identified in non-Hodgkin's lymphomas[73,74]. Corresponding to its role in normal ESCs, EZH2 was found to be essential for maintaining cancer stem cells in breast cancer[75]. EZH2 has also been found to promote cancer development when it loses its antagonistic factors[76]. In malignant rhabdoid tumours it was found that SNF5 was lost, a core subunit of the SWI/SNF complex that normally antagonises EZH2 activity[77]. These studies have suggested an oncogenic role for EZH2 however, there have been studies that also suggest a tumour-suppressive role of EZH2. Deletion, nonsense and missense mutations of EZH2 have been identified in some myeloproliferative neoplasms[78]. Loss-of-functions mutations have also been identified in T cell acute lymphoblastic leukaemia[79]. Due to the vast evidence that EZH2 can act as an oncogene in some cancers, many EZH2 inhibitors have been developed with hopes to proceed to clinical trials and provide a new treatment for many cancer patients[80]. These inhibitors include UNC1999, GSK126 and GSK343 which are used in this study.

1.3.3 EZH2 and the BASP1/WT1 complex

As mentioned previously, EZH2 was recently found to be recruited to the promoter of WT1 target genes in a BASP1-dependent manner[43]. These results are shown in Figure 1.5 where K562 cell line derivatives were used. K562 cells are a chronic myelogenous leukaemia (CML) cell line that does not express endogenous BASP1 but does express endogenous WT1. Figure 1.5 shows the ChIP assays carried out to study the recruitment of EZH2 to WT1 target gene promoters. The results show that EZH2 recruitment at WT1 target genes occurs at low levels in V-K562 cells (K562 cells transfected with an empty vector so they do not express BASP1). B-K562 cells (cells transfected with vector expressing wild-type BASP1) show enhanced recruitment of EZH2 to the promoters. G-K562 cells (cells transfected with vector expressing G2A-mutant BASP1) also show enhanced recruitment of EZH2. The results suggest that EZH2 is recruited by BASP1 in a lipid-independent manner as was referred to in Figure 1.4 and so EZH2 is thought to be responsible for placing $H3K27me^3$ marks on the promoters of BASP1/WT1 target genes.

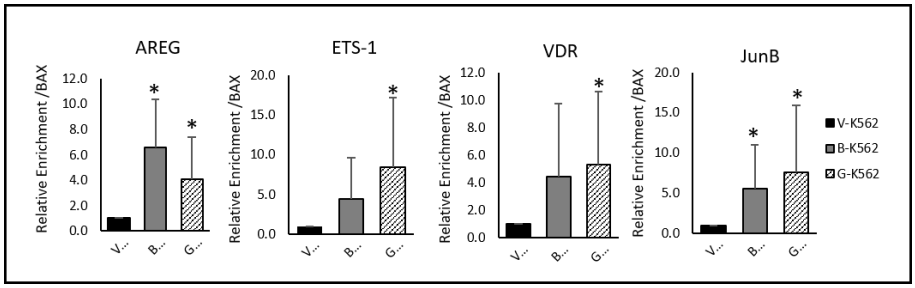

Figure 1.5: BASP1 can recruit EZH2 to WT1 target gene promoters. ChIP experiments showed that EZH2 localises to the promoter regions of WT1 target genes AREG, ETS-1, VDR and JUNB in K562 cells. Expression of BASP1 or BASP1 G2A in K562 cells enhances the recruitment of EZH2. *p<0.05 by Student's t test.[40]

1.4 Project aims

This study aims to provide a better understanding of the transcriptional regulation mechanisms carried out by the BASP1/WT1 complex. Previous data from the lab have shown that EZH2 is recruited to the promoters of WT1 target genes by BASP1 and that this coincides with the placement of H3K27me^3/H3K9me^3 marks. However, it is not known if EZH2 is involved in BASP1-mediated transcriptional repression or if its recruitment is ~~a~~ coincidental. This study aims to provide a better understanding of the potential role of EZH2 in BASP1/WT1-mediated transcriptional repression. The role of EZH2 will be investigated in the K562 cell line derivative system and in MCF7 cells, a breast cancer cell line expressing endogenous BASP1 and WT1. The first focus of this study was to determine if EZH2 has a role in the proliferation of K562 and MCF7 cells and if this was affected by the expression level of BASP1. The second focus of the study was to understand the role of EZH2 in WT1/BASP1-mediated transcriptional repression. The study makes use of specific EZH2 inhibitors, UNC1999, GSK343 and GSK126 which are S-adenosyl-L-methionine (SAM)-competitive inhibitors of EZH2[81–83]. SAM is a universal methyl donor involved in the catalytic reaction of histone methyltransferases. The effects of the EZH2 inhibitors will be studied using a group of WT1 target genes, Amphiregulin (AREG), Vitamin D Receptor (VDR), JUNB and ETS-1.

2.Methods and Materials

2.1 General Reagents

From Thermo Fisher Scientific:

Ethanol, Methanol, 4-(2-hydroxyethyl)-1-piperazineethanesulfonic acid (HEPES), Sodium Dodecyl Sulfate (SDS), Tween, Bromophenol Blue, Magnesium Chloride, Ethylene diamine tetraacetic acid (EDTA), Tris Ammonium Persulfate, Glycerol, Glycine, 37% Formaldehyde, Tris Acetate-EDTA (TAE), Ammonium Persulfate (APS)

From Sigma Life Science:

Phosphate buffered saline (PBS), Triton X-100, Lithium Chloride, Sodium Deoxycholate

Sodium Chloride and Potassium Chloride are from VWR Chemicals. Nonidet P-40 (NP-40) is from Millipore. Dithiotreitol (DTT) is from Santa Cruz Biotechnology. 30% Acrylamide/Bis Solution is from BIO-RAD. Tetramethylethylenediamine (Temed) is from Flowgen Bioscience. Dimethyl Sulfoxide (DMSO) is from Corning Mediatech.

2.2 Tissue Culture

Stable K562 cell lines were previous prepared by transfecting with pc-DNA3 plasmids that were either empty or driving expression of wtBASP1 as described previously by Goodfellow et al, 2011[25]. Cells were maintained in Rosewell Park Memorial Institute (RPMI) 1640 media supplemented with 10% Foetal Bovine Serum (FBS), 1% Penicillin-Streptomycin (Pen-Strep) and 1% L-Glutamine, all purchased from Life Technologies Inc.

Stable MCF7 cell lines were previously prepared by transfecting with pSilencer plasmids expressing either shNEGATIVE or shBASP1 as described previously by Marsh et al, 2017[33]. Cells were maintained in Dulbecco Modified Eagle Medium (DMEM) supplemented with 10% FBS, 1% Pen-Strep and 1% L-Glutamine, all purchased from Life Technologies Inc. Positive transfected cells were selected with 1mg/ml G418 (Sigma-Aldrich). Cells were kept at 37°C with 95% humidity and 5% CO_2.

2.3 EZH2 Inhibitors

UNC1999 was purchased from Cell Signalling Technology and a stock solution of 5mM in DMSO was made. UNC1999 was used at 3μM concentration.

GSK343 was purchased from APExBIO and a stock solution of 5mM in DMSO was made. GSK343 was used at 5μM concentration.

GSK126 was purchased from Adoq Bioscience and a stock solution of 5mM in DMSO was made. GSK126 was used at 8μM concentration.

2.4 Growth Assays

K562 cells were seeded at approximately $1x10^5$ cells/ml in 10ml RPMI media. Cells were treated with either 3μM UNC1999, 5μM GSK343, 8μM GSK126 or the equivalent volume of DMSO. Cells were counted every 24 hours for 5 days by mixing 10μl of cells with 10μl Trypan Blue (Invitrogen). Cells were counted using the Countess automated cell counter machine (Invitrogen).

2.5 Colony Formation Assays

MCF7 cells were seeded in 6-well plates at approximately 1000 cells in 2ml DMEM media. Cells were treated with single and double concentrations of UNC1999 (3μM/6μM), GSK343 (5μM/10μM) or GSK126 (8μM/16μM) or the equivalent volume of DMSO and left for 12 days. Media was replaced every 3 days. At 12 days, the media was removed, cells were washed once in 1ml PBS and then left for 10 minutes in 1ml Methanol (Fisher Scientific). Methanol was then removed and 0.5ml of 0.1% Crystal Violet (Sigma Life Science) was added for 5 minutes. 0.1% Crystal Violet was made by mixing 1ml 1% Crystal Violet, 3ml Methanol and 6ml H2O. Crystal Violet was then washed off and the number of colonies formed was counted as well as their size.

2.6 Nuclear Extracts

Formatted: Heading 2

K562 cells were collected, washed in 1ml of PBS per plate and centrifuged at 400g for 2 minutes. MCF7 cells were scraped off in 1ml PBS and centrifuged at 1000g for 2 minutes. PBS was removed and cells were resuspended in 1 estimated packed cell volume (PCV) of Nuclear Extract 1 (NE1) buffer and left on ice for 15 minutes. NE1 buffer contains 10mM Hepes pH 8, 1.5mM $MgCl_2$, 10mM KCl, 1mM DTT. Cells were then taken up in a 1ml syringe that had been pre-washed with NE1 buffer and

forced out through a 23-gauge needle. This process was repeated 4 times. Cells were then centrifuged at 17,000g for 30 seconds, resuspended in 2/3 PCV of Nuclear Extract 2 (NE2) buffer and placed on a rotator at 4°C for 30 minutes. NE2 contains 20mM Hepes pH 8, 1.5mM $MgCl_2$, 25% (v/v) Glycerol, 420mM NaCl, 0.2mM EDTA, 1mM DTT and 0.5mM Phenylmethylsulfonyl fluoride (PMSF). Cells were then centrifuged at 17,000g for 5 minutes and the supernatant was collected as the nuclear extract.

2.7 Western Blotting

SDS-PAGE gels were made up of a 10% (w/v) acrylamide resolving gel and a 4.5% (w/v) acrylamide stacking gel. The gel was then placed in a BIO-RAD Mini-Protean Tetra system gel tank (BIORAD) and the tank was filled with SDS-PAGE buffer which contains 25mM Tris pH 8.3, 192mM Glycine and 0.1% (w/v) SDS. 10-20ul of nuclear extract was loaded into the wells as well as 2µl of Spectra BR marker (Thermo Scientific) mixed with 5µl loading dye and 14 µl H2O. The gel was resolved at 150V for approximately 1 hour. The proteins were then transferred onto a methanol activated Immobilon-P membrane (Merck) in transfer buffer containing 25mM Tris pH 8.3, 192mM Glycine, 10% (v/v) methanol, using a semi-dry transfer cell (BIORAD) running at 25V for 40 minutes. Membrane was then blocked for 1 hour in 15ml blocking buffer containing 150mM NaCl, 20mM Tris pH 7.5. 0.1% (v/v) Tween and 5% (w/v) dried milk. After blocking, the membrane was left at 4°C overnight with the appropriate antibody (Table 2.1) diluted in blocking buffer. The following day the membrane was washed 5 times with 10-15ml blocking buffer for 5 minutes each time. Then the membrane was left rocking for 1 hour at room temperature with the appropriate secondary antibody (Table 2.1) diluted in blocking buffer. The same washes were repeated before adding Pierce ECL Western Blotting Substrate (Thermo Scientific). Protein detection was then done on CL-X Posure™ Films (Thermo Scientific) using a Konica Minolta™ SRX-101A Film Processor.

Antibody	Species	Dilution	Source
BASP1	Rabbit	1:2000	Pacific Immunology, California
WT1	Rabbit	1:2000	Pacific Immunology, California
GAPDH	Mouse	1:10000	Merck Millipore
Anti-Rabbit HRP	Goat	1:10000	Jackson ImmunoResearch Laboratories
Anti-Mouse HRP	Goat	1:10000	Jackson ImmunoResearch Laboratories

Table 2.1: Antibodies used for Western Blotting

2.8 Gene Expression

RNA was extracted from K562 and MCF7 cell pellets using a RNeasy Mini Kit (Qiagen) and following the manufacturer's instructions. RNA concentration was then measured using a NanoDrop Lite (Thermo Scientific) and diluted to 1ug/ul.

cDNA was prepared using an iScript cDNA synthesis kit (BIORAD) following the manufacturer's instructions and then using a Techne PCR machine set at 25°C for 5 minutes, 42°C for 30 minutes and 85°C for 5 minutes the cDNA was prepared.

q-PCR reactions were set up consisting of 2µl cDNA (prepared as described above for RNA extraction and cDNA preparation), 10 µl SYBR Green (BIORAD), 7µl H_2O and 1 µl Primer stock. Primer stocks for each gene were made up with 50ng/µl forward primer and 150ng/µl reverse primer (Table 2.2). The q-PCR machine was set at 95°C for 3 minutes followed by 40 cycles to 95°C for 20 seconds, 60°C for 30 seconds and 72°C for 30 seconds. To also plot a melt curve, the q-PCR machine was set at 95°C for 10 seconds and then 65°C for 5 seconds with the temperature then rising by 0.5°C every 5s followed by a plate read each time until the temperature reaches 95°C. The melt curves are shown in section 6.1. For AREG, annealing temperature was set at 50°C.

PRIMERS	Forward Primer 5'-3'	Reverse Primer 5'-3'
GAPDH	ACAGTCAGCCGCATCTTCTT	ACGACCAAATCCGTTGACTC
AREG	TGGATTGGACCTCAATGACA	ACTGTGGTCCCCAGAAAATG
VDR	CTGACCCTGGAGACTTTGAG	TTCCTCTGCACTTCCTCA
JUNB	TGGTGGCCTCTCTCTACACGA	GGGTCGGCCAGGTTGAC
ETS1	AAACTTGCTACCATCCCGTACGT	ATGGTGAGAGTCGGCTTGAGAT

Table 2.2: Primers used for quantitative PCR

2.9 Chromatin Immunoprecipitation (ChIP)

ChIP Buffers:

IP Buffer: 150mM NaCl, 50mM Tris-HCl pH 8, 5mM EDTA, 0.5% (v/v) NP-40, 1% (v/v) Triton X-100

High Salt Buffer: 500mM NaCl, 50mM Tris-HCl pH 8, 5mM EDTA, 0.5% (v/v) NP-40, 1% (v/v) Triton X-100

LiCl Buffer: 10mM Tris-HCl pH 8, 250mM LiCl, 1mM EDTA, 1% (v/v) NP-40, 1% (w/v) Sodium Deoxycholate

TE Buffer: 10mM Tris-HCl pH 8, 1mM EDTA

PK Buffer: 125mM Tris-HCl pH 8,10mM EDTA, 150mM NaCl, 1% (w/v) SDS

K562 cells were harvested and resuspended in Phosphate-buffered saline (PBS) to obtain a concentration of $1x10^6$/ml. The cells were then cross-linked by incubating with 40µl/ml of PBS of 37% (v/v) formaldehyde for 15 minutes at room temperature on a rocker. The cells were then quenched with 141µl/ml of PBS of 1M glycine and left for 5 minutes at room temperature on a rocker. The cells were then centrifuged at 2000g for 5 minutes and the cell pellet was resuspended in 5ml of cold PBS. The cells were centrifuged again and resuspended in 1ml IP buffer containing set III protease inhibitors (Calbiochem) and left on ice for 15 minutes to lyse. The lysed cells were then centrifuged at 2000g for 5 minutes at 4°C and resuspended in 1ml IP buffer containing set III protease inhibitors.

The cells were then sonicated using a QSonica Q500 sonicator set at 50% amplitude for 3 seconds ON 2 seconds OFF pulses. This was repeated 16 times for each tube

of cells. The cells were kept on ice between pulses. The sonicated cells were then centrifuged at 12000g for 10 minutes at 4°C and the supernatant was collected and mixed with 10µl/ml Mag-G beads (Life Technologies) and left to rotate for 1 hour at 4°C to preclear the chromatin.

Successful sonication resulting in the production of 200-500bp fragment was confirmed by taking a small sample of the sheared chromatin and de-crosslinking it by incubating at 37°C with 30µl PK buffer and 1 µl RNAase A (Abcam) from the ab185913 High-Sensitivity ChIP kit, as per manufacturer's instructions, for 30 minutes. After 30 minutes 1µl of 20mg/ml Proteinase K (Ambion #AM2546) was added and samples left at 62°C for 2 hours to complete de-crosslinking. Samples were then loaded onto a 1.5% agarose gel and resolved at 100V for 45 minutes in 1xTris-acetate-EDTA (TAE) buffer to confirm fragmentation.

Microtubes containing 600µl IP buffer, 10µl Mag-G beads, 1µl of 10mg/ml acetylated BSA (Sigma) and the appropriate antibody (Table 2.3) were previously prepared for each ChIP sample and rotated at 4°C for at least 4 hours or overnight. 200 µl of the precleared samples was then added to each antibody microtube and left to rotate at 4°C overnight. 2% of the precleared samples was kept at -20°C for later use.

The next day, the immunoprecipitated samples were magnetised to remove the supernatant and then washed in 1ml of IP buffer and left on ice for 3 minutes. Samples were then washed in the same way with 1ml High Salt, with 1ml LiCl buffer and TE buffer. Samples, including the 2% inputs, were then resuspended in 100µl PK buffer and left at 65°C overnight. The samples were then incubated at 55°C for 3-4 hours, with 1µl 20mg/ml Proteinase K. The samples were centrifuged at 17000g for 5 minutes and the DNA in the supernatant purified using a Qiaquick PCR purification kit according to the manufacturer's instructions. The eluted DNA was then heated at 95°C for 10 minutes and prepared for q-PCR as described in section 2.8 using the suitable primers (Table 2.4). The q-PCR machine was set at 95°C for 3 minutes followed by 40 cycles of 95°C for 10 seconds, 60°C for 10 seconds and 72°C for 30 seconds. To also plot a melt curve the q-PCR machine was set up as detailed in section 2.8. The melt curves are shown in section 6.3.

ChIP Antibody	Species	Volume per IP	Source
H3K9ac	Rabbit	4 µl	Abcam #ab10812
H3K27me^3	Mouse	4µl	Abcam #ab8898
Normal IgG	Rabbit	1µl	Cell Signalling #2729
Normal IgG	Mouse	1µl	Millipore #12-371

Table 2.3: Antibodies used for ChIP

ChIP Primer	Forward Primer 5'-3'	Reverse Primer 5'-3'
18S	GTAACCCGTTGAACCCCATT	CCATCCAATCGGTAGTAGCG
AREG	TTTAAGTTCCACTTCCTCTCA	GGTGTGCGAACGTCTGTA
JUNB	GGTCCTGGTATTTGTCCCAG	CTCGCGTCACTGTCAGGAAG
VDR	CACCTGGCTCAGGCGTCC	GCCAGGAGCTCCGTTGGC
ETS-1	CCTAAAGAGGAGGGGAGAGC	AGGGGAAGTTGGCACTTTG

Table 2.4: Primers used for ChIP

3.Results

3.1 The effect of EZH2 inhibition on cell growth

3.1.1 Verifying the absence and presence of BASP1

The first step of this study was to verify that the cell lines had been stably transfected resulting in the production of two derivative cell lines, the V-K562 cells and the B-K562 cells. K562 cells express endogenous WT1 but do not express BASP1 so the cells had previously been transfected with either an empty vector to produce the V-K562 cells or with a vector expressing wild type BASP1 (wtBASP1) to produce the B-K562 cells. Western blots were carried out to confirm the absence of BASP1 in V-K562 cells and the presence of BASP1 in B-K562 cells by preparing nuclear extracts from the cells. BASP1 was detected at approximately 52kDa only in the extract prepared from B-K562 cells as shown in Figure 3.1.

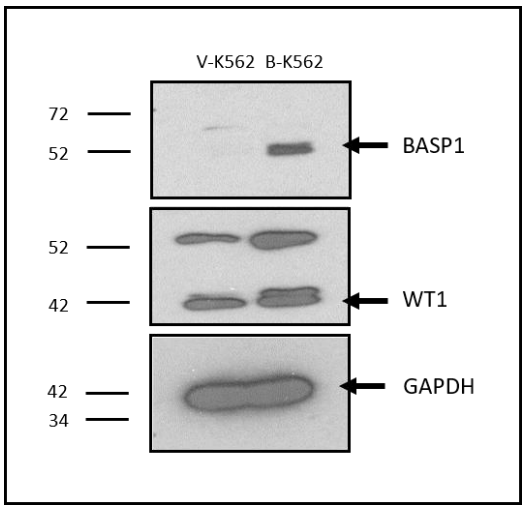

Figure 3.1: Immunoblots showing the expression of BASP1 in K562 cells. Immunoblots were probed for BASP1 and WT1 for V-K562 and B-K562 cells. GAPDH is shown as a loading control. Molecular weight markers (kDa) are shown at the left of each immunoblot.

Figure 3.1 also shows the expression of endogenous WT1 in K562 cells. The major forms of WT1 migrate as a doublet due to the -17AA and +17AA forms. The B-K562 cells appear to express more of the +17AA isoform compared to the V-K562 cells. This was not observed in previous studies of these cells[25]. It is notable that the

slower migrating immunoreactive band in the WT1 blot is also enhanced in the B-K562 cells compared to the V-K562 cells. This immunoreactive band may be a form of WT1 that arises from an upstream translation start site[3].

The second step of the study was to verify that the treatment of K562 cells with the EZH2 inhibitors UNC1999, GSK343 and GSK126 does not alter the expression level of BASP1. V-K562 and B-K562 cells were therefore treated with either DMSO or an EZH2 inhibitor for 72 hours and nuclear extracts were prepared and resolved by SDS-PAGE followed by Western blotting to detect BASP1, as shown in Figure 3.2.

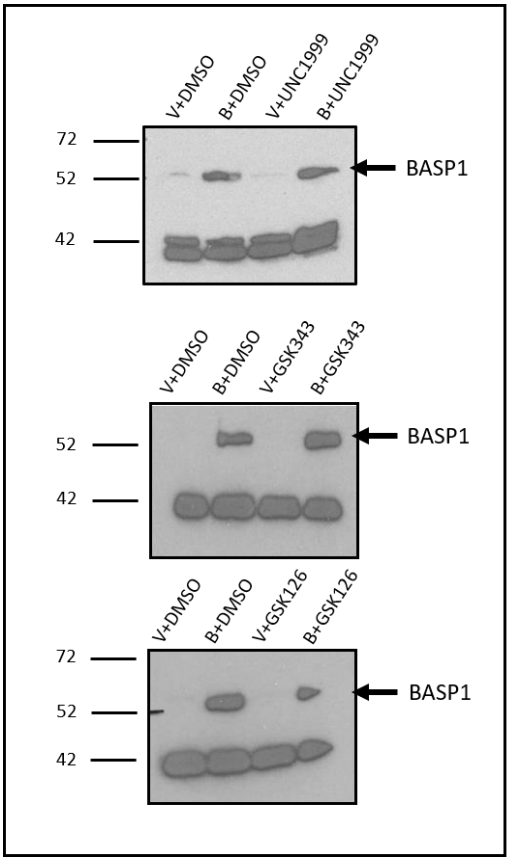

Figure 3.2: Immunoblots showing the expression of BASP1 in K562 cells following treatment with EZH2 inhibitors. Immunoblots probed with BASP1 for V-K562 and B-K562 cells treated with DMSO, UNC1999 (3µM), GSK343 (5µM) or GSK126 (8µM). Molecular weight markers (kDa) are shown at the left of each immunoblot.

Figure 3.2 shows that treatment of K562 cells with UNC1999, GSK343 or GSK126 does not alter the expression level of BASP1. BASP1 is expressed only in B-K562 cells and not in V-K562 cells for cells treated with DMSO or one of the inhibitors. The faster migrating band expressed in all cells is non-specific band and acts as a loading control.

A second cell line system was also used for this study, MCF7 cells. MCF7 cells express endogenous BASP1 and so were previously stably transfected with a plasmid driving the expression of either a control shRNA (shNEG) or shRNA directed against BASP1 (shBASP1) to produce two derivative cell lines[33]. The shNEG cells which express endogenous BASP1 and the shBASP1 cells where BASP1 is knocked down. Western Blots were first carried out to confirm that the cells were stably transfected as shown in Figure 3.3.

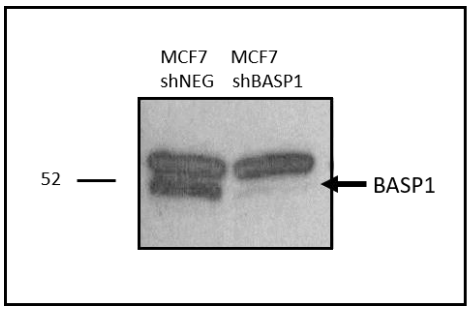

Figure 3.3: Immunoblot showing the expression of BASP1 in MCF7 cells. Immunoblot was probed for BASP1 for shNEG and shBASP1 cells. ~~GAPDH is shown as a loading control.~~ Molecular weight markers (kDa) are shown at the left of each immunoblot.

Figure 3.3 shows that BASP1 was knocked down successfully in shBASP1 cells however, no loading control was used and so to verify that the same amount of protein was loaded for both samples that need to be done. The immunoblot probed with BASP1 shows two bands close to the known migration point of BASP1. Based on previous studies from the lab, the slower migrating band is a non-specific band that has a similar molecular weight to BASP1, and the faster migrating band is BASP1 which is present in shNEG cells and knocked down in shBASP1 cells.

3.1.2 Evaluation of the effects of EZH2 inhibitors on the growth of K562 cells

Next, we wanted to study if the inhibition of EZH2 has an effect on the growth rate of K562 cells. To measure this, K562 cells were treated with either DMSO or an EZH2 inhibitor and then the number of cells was counted every 24 hours for 5 days as shown in Figure 3.4.

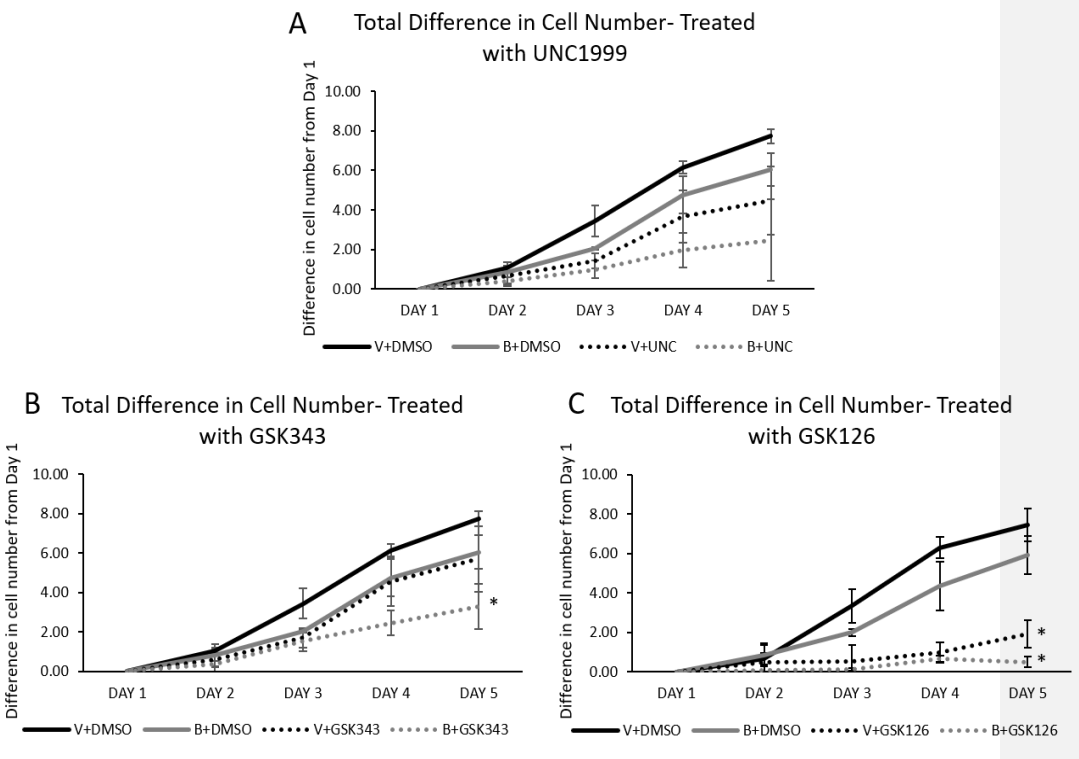

Figure 3.4: EZH2 inhibition effect on the growth of K562 cells. Growth assays were carried out on the K562 cell line derivatives following treatment with either DMSO or (A) UNC1999 (~~3~~6μM), (B) GSK343 (5μM) and (C) GSK126 (8μM). The number of cells was measured every 24 hours for 5 days. The y-axis shows the difference in cell number from Day1 (Dayx-Day1). Significant difference between the effect of DMSO and the EZH2 inhibitor is indicated by *. (B) Significant difference between B+DMSO and B+GSK343 (p value=0.0278). (C) Significant difference between V+DMSO and V+GSK126 (p value=0.0009) and between B+DMSO and B+GSK126 (p value-=0.0008)

The three graphs in Figure 3.4 show that V-K562 cells grow faster than B-K562 cells. This agrees well with previous results, that expression of BASP1 slows down K562 cell growth[1].Figure 3.4 (A) shows that when treated with UNC1999, K562

cell growth is decreased in both V-K562 and B-K562 cells, however this effect was not found to be significant. Figure 3.4 (B) shows that when K562 cells were treated with GSK343 there is slight decrease in the growth rate of V-K562 cells which is not significant but there is a significant decrease in growth of the treated B-K562 cells. This suggests that GSK343 only has a significant effect on the growth rate of K562 cells when BASP1 is present. Finally, Figure 3.4 (C) shows that GSK126 significantly decreases the growth rate of both V-K562 and B-K562 cells. Taken together these results suggest that, overall, the inhibition of EZH2 slows down the growth rate of K562 cells and that GSK343 appears to have a greater effect on the growth of K562 cells when BASP1 is present.

3.1.3 The effects of EZH2 inhibitors on MCF7 tumorigenicity

To determine the effect of EZH2 inhibition on MCF7 cell growth, colony formation assays were carried out where the cells were either treated with DMSO or one of the three inhibitors at two different concentrations. After 12 days the number (Figure 3.5 A) and size (Figure 3.5 B) of the colonies present was determined. The shBASP1 MCF7 cells showed both an increase in colony number (Figure 3.5 A) and average size (Figure 3.4 B) compared to shNEG MCF7 cells. These results are consistent with previous studies and are indicative of a tumour suppressor function for BASP1 in MCF7 cells[33].

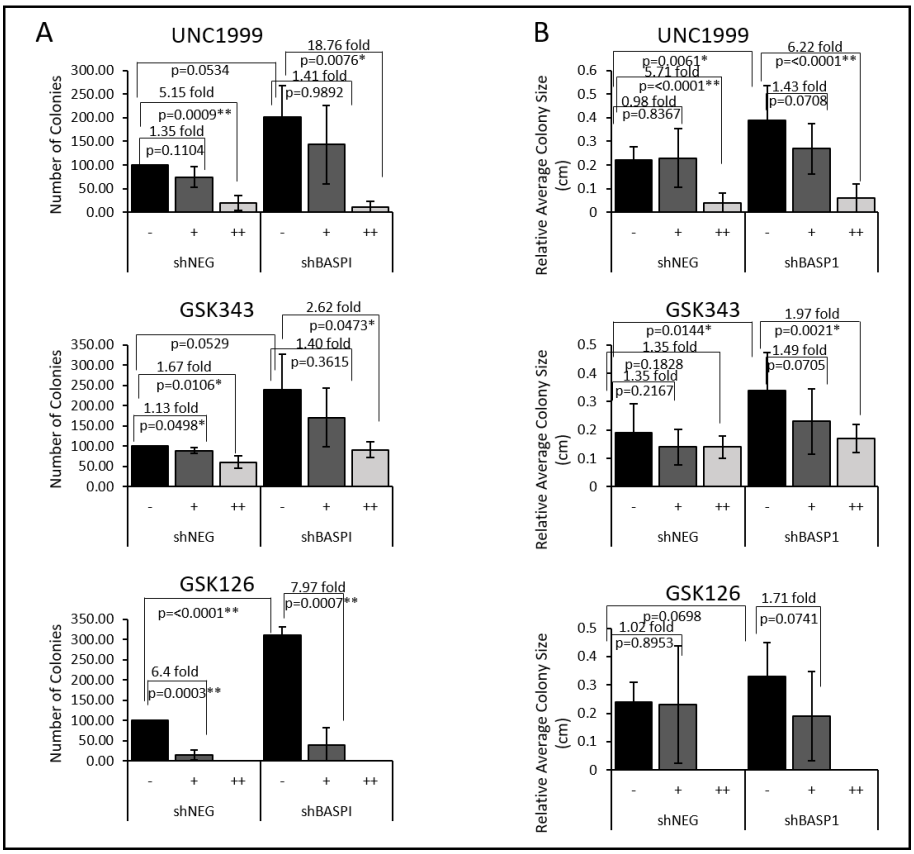

Figure 3.5: EZH2 inhibition effect on MCF7 tumorigenicity. (A) Graphs show the average number of colonies counted 12 days after MCF7 cells were treated with UNC1999 at 3µM [+] and 6µM [++], GSK343 at 5µM [+] and 10µM [++] or GSK126 8µM [+] and 16µM [++]. Cells were also treated with DMSO for a control. The number of colonies have been normalised to shNEG+DMSO=100. (B) Graphs show the relative average size of the colonies counted in cm.

Figure 3.5 A shows the average number of colonies counted after treatment with each of the EZH2 inhibitors. With all 3 inhibitors it can be seen that the number of colonies decreases as the concentration of the drug increases in both shNEG and shBASP1 cells. Figure 3.5 B shows a similar effect of the EZH2 inhibitors on colony size where it generally decreases as the inhibitor concentration increases in both shNEG and shBASP1 cells.

The UNC1999 inhibitor fails to cause a significant decrease in colony number or size when used at 3μM (+). However, treatment with UNC1999 at 6μM (++) causes a significant decrease in both colony number and size in both shNEG and shBASP1 cells. In MCF7 shBASP1 cells, 6μM UNC1999 had a greater effect in decreasing the number of colonies (~19-fold) compared to its effect in MCF7 shNEG cells where it decreases by ~5-fold. However, the effect of 6μM UNC1999 on colony size was similar in both MCF7 shNEG and MCF7 shBASP1 cells.

The GSK343 inhibitor caused a significant decrease in colony number and size for both MCF7 shNEG and shBASP1 cells when used at 10μM. It also caused a significant decrease in colony number in MCF7 shNEG cells when used at 5μM. The effects of both 5μM and 10μM GSK434 was similar in both shNEG MCF7 and shBASP1 MCF7 cells.

The GSK126 inhibitor appears to be the most potent of the 3 compounds in reducing colony formation of the MCF7 cell derivatives. At 16μM the inhibitor prevents the formation of any colonies. When used at [8μM], GSK126 caused a highly significant decrease in the number of colonies present in both shNEG and shBASP1 cells, however it did not significantly affect the size of the colonies. Taken together these results suggest that inhibition of EZH2 reduces the tumorigenicity of the MCF7 cell derivatives by preventing the formation of colonies. While the effects were generally observed to be BASP1-independent, UNC1999 was a more effective inhibitor of MCF7 colony formation in the absence of BASP1.

3.2 The effect of EZH2 inhibition on gene expression

3.2.1 RNA analysis of K562 cells following EZH2 inhibition

After establishing the stable transfection of the cells and studying the effect of EZH2 inhibition on growth, the next step was to study its effects on transcriptional regulation by BASP1/WT1. Four known WT1 target genes were selected to analyse because these had been studied before in K562 cells by our lab[3,28]. The 4 genes are AREG, VDR, JUNB and ETS-1. To study the effect of EZH2 inhibition on gene expression, K562 cell derivatives were treated with either one of the inhibitors or the equivalent amount of DMSO for 72 hours. RNA was then extracted from the cells, used to produce cDNA and qPCR was carried out to measure the expression of

each of the four genes. GAPDH expression was also measured because it is not a WT1 target gene, so it was used as a control.

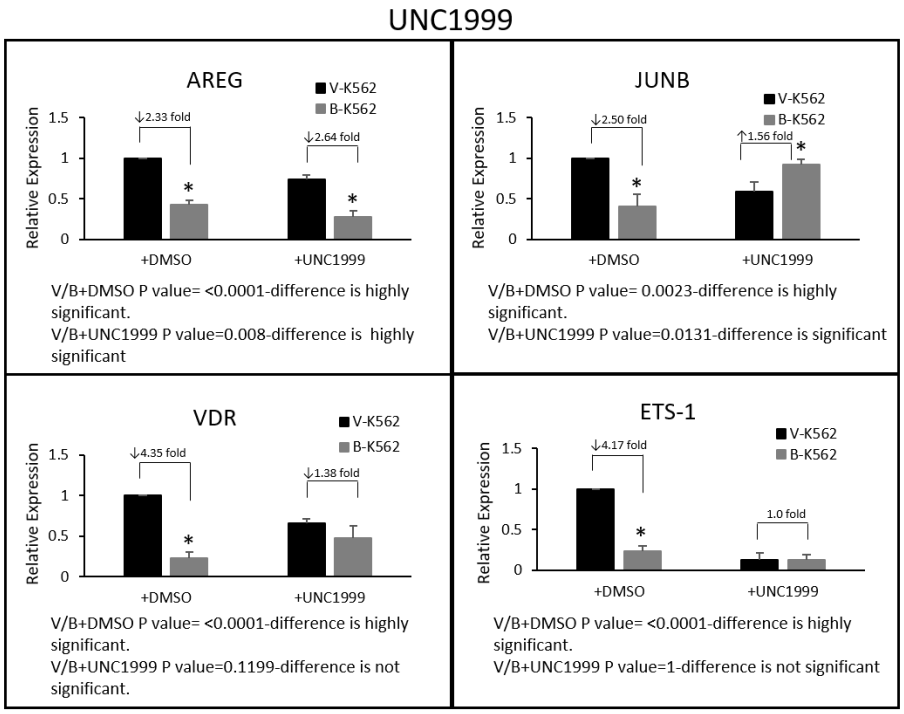

Figure 3.6: RNA analysis of K562 cells after treatment with UNC1999. The relative expression of AREG, JUNB, VDR and ETS1 compared to GAPDH in V-K562 and B-K562 cells treated with 3µM of the EZH2 inhibitor UNC1999 or the equivalent volume of DMSO. Significant differences indicated with * for p <0.05 using a Student's t test.

Figure 3.6 shows the relative expression of AREG, JUNB, VDR and ETS-1 following the treatment of V-K562 and B-K562 cells with the UNC1999 EZH2 inhibitor. Previous studies showed that the presence of BASP1 causes repression of these genes, as is seen in the V-K562 and B-K562 cells treated with DMSO here[16]. AREG expression is significantly 2.33-fold repressed by BASP1 in untreated B-K562 cells compared to V-K562 cells. AREG is also repressed by UNC1999, as there is decreased gene expression in both treated V-K562 and B-K562 cells compared to untreated V-K562 and B-K562 cells. In the presence of UNC1999, AREG is

significantly 2.64-fold repressed by BASP1 in treated B-K562 cells compared to treated V-K562 cells. This suggests that EZH2 inhibition by UNC1999 does not affect the ability of BASP1 to repress transcription of AREG. JUNB expression is significantly 2.5-fold repressed by BASP1 in untreated B-K562 cells compared to V-K562 cells. JUNB is only repressed by UNC1999 in the absence of BASP1 as there is a decrease in JUNB expression in treated V-K562 cells compared to untreated V-K562 cells and an increase in JUNB expression in treated B-K562 cells compared to untreated B-K562 cells. In the presence of UNC1999, JUNB is significantly 1.56-fold overexpressed by BASP1 in treated B-K562 cells compared to treated V-K562 cells. This suggests that BASP1 needs EZH2 to repress the transcription of JUNB. VDR expression is significantly 4.53-fold repressed by BASP1 in untreated B-K562 cells compared to V-K562 cells. VDR is only repressed by UNC1999 in the absence of BASP1 as there is a decrease in VDR expression in treated V-K562 cells compared to untreated V-K562 cells and an increase in VDR expression in treated B-K562 cells compared to untreated B-K562 cells. In the presence of UNC1999, there is no significant change in VDR expression in treated B-K562 compared to treated V-K562 cells. This suggests that BASP1 needs EZH2 to repress the transcription of VDR. ETS-1 expression is significantly 4.17-fold repressed by BASP1 in untreated B-K562 cells compared to V-K562 cells. ETS-1 is also repressed by UNC1999, as there is decreased gene expression in both treated V-K562 and B-K562 cells compared to untreated V-K562 and B-K562 cells. In the presence of UNC1999, there is no significant change in ETS-1 expression in treated B-K562 cells compared to treated V-K562 cells. This suggests that BASP1 needs EZH2 to repress the transcription of ETS-1. Taken together these data demonstrate that the treatment of K562 cells with UNC1999 abolishes the BASP1-dependent transcriptional repression of JUNB, VDR and ETS-1 but not AREG.

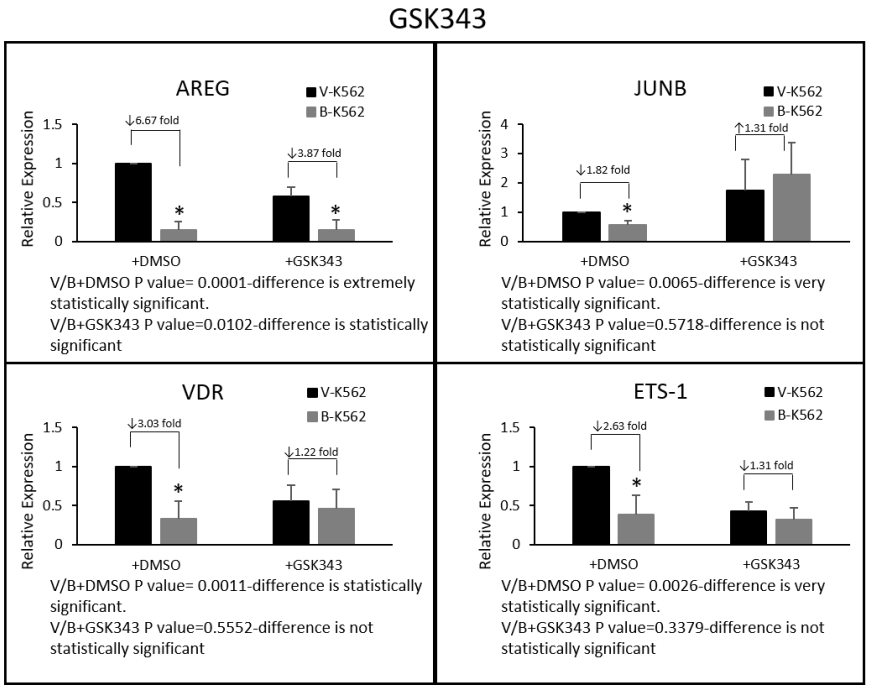

Figure 3.7: RNA analysis of K562 cells after treatment with GSK343. The relative expression of AREG, JUNB, VDR and ETS1 in V- and B-K562 cells treated with 5µM of the EZH2 inhibitor GSK343 or the equivalent volume of DMSO. Significant differences indicated with * for $p < 0.05$ using a Student's t test.

Figure 3.7 shows the relative expression of AREG, JUNB, VDR and ETS-1 following the treatment of V-K562 and B-K562 cells with the GSK343 EZH2 inhibitor. AREG expression is significantly 6.67-fold repressed by BASP1 in untreated B-K562 cells compared to V-K562 cells. AREG is also repressed by GSK343, as there is decreased gene expression in both treated V-K562 and B-K562 cells compared to untreated V-K562 and B-K562 cells. In the presence of GSK343, AREG is significantly 3.87-fold repressed by BASP1 in treated B-K562 cells compared to treated V-K562 cells. This suggests that EZH2 inhibition by GSK343 does not affect the ability of BASP1 to repress transcription of AREG. JUNB expression is significantly 1.82-fold repressed by BASP1 in untreated B-K562 cells compared to V-K562 cells. JUNB is not repressed by GSK343 as there is an increase in JUNB expression in treated V-K562 cells compared to untreated V-K562 cells and an

increase in JUNB expression in treated B-K562 cells compared to untreated B-K562 cells. In the presence of GSK343, JUNB is 1.31-fold overexpressed by BASP1 in treated B-K562 cells compared to treated V-K562 cells. This suggests that BASP1 needs EZH2 to repress the transcription of JUNB. VDR expression is significantly 3.03-fold repressed by BASP1 in untreated B-K562 cells compared to V-K562 cells. VDR is only repressed by GSK343 in the absence of BASP1 as there is a decrease in VDR expression in treated V-K562 cells compared to untreated V-K562 cells and an increase in VDR expression in treated B-K562 cells compared to untreated B-K562 cells. In the presence of GSK343, there is no significant change in VDR expression in treated B-K562 compared to treated V-K562 cells. This suggests that BASP1 needs EZH2 to repress the transcription of VDR. ETS-1 expression is significantly 2.63-fold repressed by BASP1 in untreated B-K562 cells compared to V-K562 cells. ETS-1 is also repressed by GSK343, as there is decreased gene expression in both treated V-K562 and B-K562 cells compared to untreated V-K562 and B-K562 cells. In the presence of GSK343, there is no significant change in ETS-1 expression in treated B-K562 cells compared to treated V-K562 cells. This suggests that BASP1 needs EZH2 to repress the transcription of ETS-1. Thus, the treatment of K562 cells with GSK343 abolishes the BASP1-dependent transcriptional repression of JUNB, VDR and ETS-1 but not AREG.

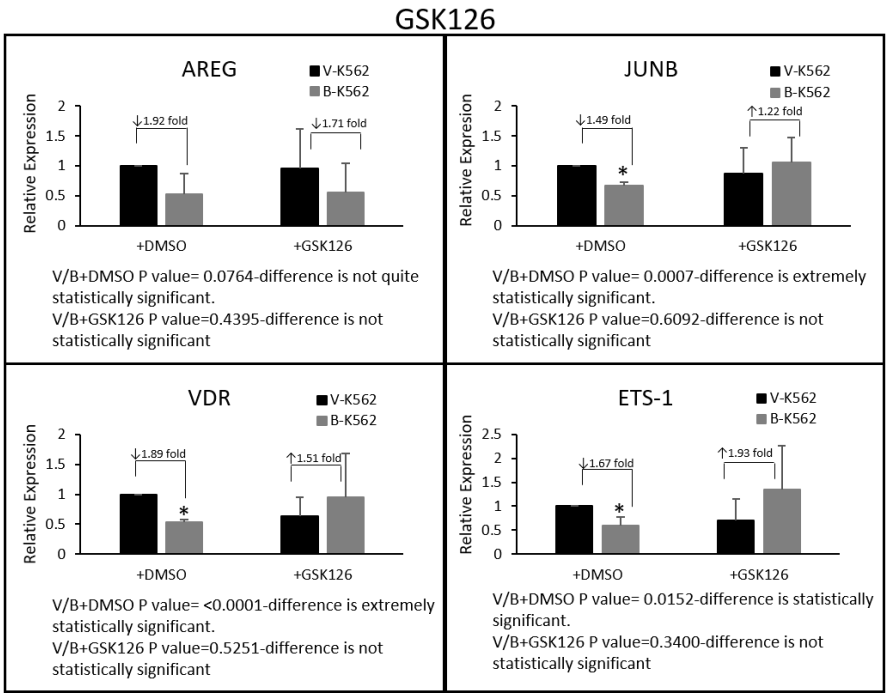

Figure 3.8: RNA analysis of K562 cells after treatment with GSK126. The relative expression of AREG, JUNB, VDR and ETS1 in V- and B-K562 cells treated with 8μM of the EZH2 inhibitor GSK126 or the equivalent volume of DMSO. Significant differences indicated with * for p <0.05 using a Student's t

Figure 3.8 shows the relative expression of AREG, JUNB, VDR and ETS-1 following the treatment of V-K562 and B-K562 cells with the GSK126 EZH2 inhibitor. AREG expression is 1.92-fold repressed by BASP1 in untreated B-K562 cells compared to V-K562 cells. AREG is only repressed by GSK126 in the absence of BASP1 as there is a decrease in AREG expression in treated V-K562 cells compared to untreated V-K562 cells and a small increase in AREG expression in treated B-K562 cells compared to untreated B-K562 cells. In the presence of GSK126, AREG is 1.71-fold repressed by BASP1 in treated B-K562 cells compared to treated V-K562 cells. The decrease in AREG expression in untreated B-K562 cells compared to untreated V-K562 cells and the decrease between treated B-K562 cells and treated V-K562 cells is not significant. This suggests that EZH2 inhibition by GSK126 does not affect the ability of BASP1 to repress transcription of AREG. JUNB

expression is significantly 1.49-fold repressed by BASP1 in untreated B-K562 cells compared to V-K562 cells. JUNB is only repressed by GSK126 in the absence of BASP1 as there is a decrease in JUNB expression in treated V-K562 cells compared to untreated V-K562 cells and an increase in JUNB expression in treated B-K562 cells compared to untreated B-K562 cells. In the presence of GSK126, JUNB is 1.22-fold overexpressed by BASP1 in treated B-K562 cells compared to treated V-K562 cells. This suggests that BASP1 needs EZH2 to repress the transcription of JUNB. VDR expression is significantly 1.89-fold repressed by BASP1 in untreated B-K562 cells compared to V-K562 cells. VDR is only repressed by GSK126 in the absence of BASP1 as there is a decrease in VDR expression in treated V-K562 cells compared to untreated V-K562 cells and an increase in VDR expression in treated B-K562 cells compared to untreated B-K562 cells. In the presence of GSK126, VDR is 1,51-fold overexpressed by BASP1 in treated B-K562 cells compared to treated V-K562 cells. This suggests that BASP1 needs EZH2 to repress the transcription of VDR. ETS-1 expression is significantly 1.67-fold repressed by BASP1 in untreated B-K562 cells compared to V-K562 cells. ETS-1 is only repressed by GSK126 in the absence of BASP1 as there is a decrease in ETS-1 expression in treated V-K562 cells compared to untreated V-K562 cells and an increase in ETS-1 expression in treated B-K562 cells compared to untreated B-K562 cells. In the presence of GSK126, there ETS-1 is 1.93-fold overexpressed by BASP1 in treated B-K562 cells compared to treated V-K562 cells. This suggests that BASP1 needs EZH2 to repress the transcription of ETS-1. Thus, the treatment of K562 cells with GSK126 abolishes the BASP1-dependent transcriptional repression of JUNB, VDR and ETS-1 but not AREG.

Taken together, the results analysing RNA expression using the inhibitors UNC1999, GSK343 and GSK126 show that BASP1 requires EZH2 to carry out its transcriptional repression activities on JUNB, VDR and ETS-1. The results also show that BASP1 does not need EZH2 to repress the expression of AREG. This suggests that BASP1 can act in different ways on different genes to carry out its role as a transcriptional repressor.

3.2.2 ChIP analysis of K562 cells following EZH2 inhibition

Following RNA analysis experiments, ChIP experiments were carried out to test for the presence of H3K27me^3 repressive marks and H3K9ac activation marks on the promoters of WT1 target genes. For ChIP, the AREG and VDR genes were analysed following 48-hour treatment of V-K562 and B-K562 cells with UNC1999 or the equivalent volume of DMSO. EZH2 is known to be responsible for placing H3K27me^3 marks on gene promoters so by treating the cells with an EZH2 inhibitor we can study if BASP1 loses its ability to repress genes in the presence of UNC1999 due to failure of EZH2 to place H3K27me^3 marks. H3K9ac marks are not removed by EZH2 so inhibition of EZH2 should not have a direct effect on H3K9ac marks. The presence of these marks was also measured on BAX which is not a WT1 target gene and thus acts as a control.

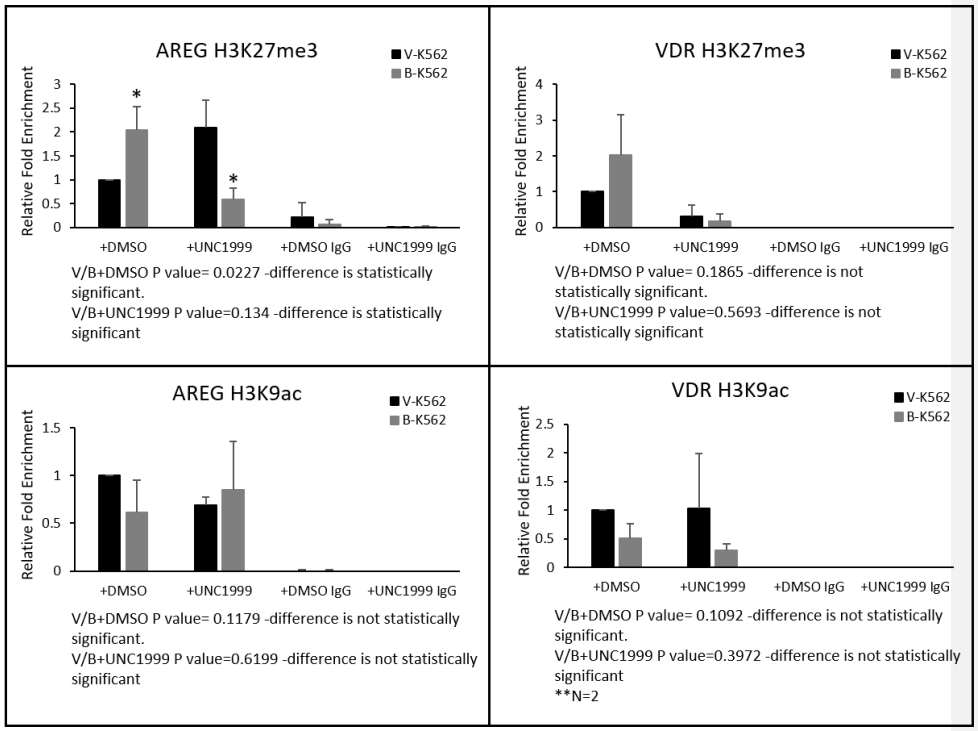

Figure 3.9: ChIP analysis of K562 cells after treatment with UNC1999. The relative fold enrichment of H3K27me^3 marks and H3K9ac marks compared to BAX on AREG and VDR gene promoters in V- and B-K562 cells treated with 3µM of the EZH2 inhibitor UNC1999 or the equivalent volume of DMSO for 48 hours. Significant differences indicated with * for $p < 0.05$ using a Student's t test.

Figure 3.9 shows the relative fold enrichment of H3K27me^3 and H3K9ac marks at AREG and VDR gene promoters. For AREG, it was observed as expected that in untreated B-K562 cells there is a significant increase in H3K27me^3 marks and a decrease in H3K9ac marks compared to untreated V-K562 cells, corresponding with AREG being repressed (however, the latter was not found to be significant). When the cells are treated with UNC1999, there is a significant decrease in H3K27me^3 marks in treated B-K562 cells compared to treated V-K562 cells showing that the inhibition of EZH2 prevents H3K27me^3 marks from being placed. There is no significant change in H3K9ac marks on the promoter of AREG between treated V-K562 and B-K562 cells, further showing that EZH2 is not involved in the process of removing H3K9ac marks. For VDR, there is an increase in H3K27me^3 and a

decrease in H3K9ac marks in untreated B-K562 cells compared to untreated V-K562 cells, however these changes were not significant. After treatment with UNC1999 there is a decrease of H3K27me^3 marks in both treated V-K562 and B-K562 cells suggesting that EZH2 plays a role in placing this histone modification. There is also a slight decrease in the level of H3K27me^3 marks between treated V-K562 and B-K562 cells which is in contrast to the BASP1-dependent increase in H3K27me^3 in untreated cells. Although these changes were not found to pass a significance test, they are consistent with BASP1-dependent H3K27 methylation via EZH2. There is also no significant change in the levels of H3K9ac marks between treated B-K562 and V-K562 cells, as was observed at the AREG promoter.

Taken together these results suggest that EZH2 is required to place H3K27me^3 marks on the AREG promoter and that this occurs in a BASP1-dependent manner. EZH2 is also required to place H3K27me^3 marks on the VDR promoter and although the data are consistent with BASP1-dependence, the changes were not found to be significant.

4.Discussion

4.1 BASP1 as a growth regulator

The aim of this study was to establish whether EZH2 is directly involved in the BASP1/WT1 transcriptional repressive complex to better understand the mechanism by which this complex can repress its target genes. BASP1 has been found to be involved in many types of cancer both as a TSG and as an oncogene therefore, another part of this study was to determine whether EZH2 can affect the behaviour of BASP1 in cancer. Using three EZH2 inhibitors (UNC1999, GSK343 and GSK126) and two cell lines (K562 cells and MCF7 cells), growth assays were carried out. In K562 cells, BASP1 has been previously shown to act as a TSG gene where the expression of BASP1 in K562 cells results in a decreased growth rate of these leukaemic cells[25]. A similar effect is seen in MCF7 cells were the knockdown of BASP1 results in an increased growth rate of the cells[33]. In these two cell lines BASP1 is suggested to have a TSG role.

In K562 cells, treatment with EZH2 inhibitors further decreased the cells' growth rate. Previous studies have suggested that EZH2 can also be involved in many cancers as both a TSG and an oncogene and so its inhibition results in a decreased growth rate in both V-K562 and B-K562 cells[67]. UNC1999 and GSK343 had a greater effect in decreasing cell growth in the B-K562 cells compared to the V-K562 cells. These results suggest that EZH2 has an oncogenic role in these cells and when inhibited, the role of BASP1 as a TSG can be enhanced to further repress tumour growth. With GSK126, both V-K562 and B-K562 cell growth is significantly decreased when the cells are treated with the inhibitor. These results suggest that GSK126 might not act in a BASP1-dependent manner to decrease cell growth. Since GSK126 inhibits EZH2 by the same mechanism as GSK343 they were expected to cause similar effects. More experiments are needed with a lower concentration of GSK126 to confirm this.

In MCF7 cells, colony formation assays showed that treatment of the cells with the inhibitors resulted in a decrease in both colony number and size suggesting that the inhibition of EZH2 results in decreased tumorigenicity of these cells. Colony number and size is higher in shBASP1 cells compared to shNEG cells correlating with BASP1 having a tumour suppressive role. The effect of EZH2 inhibition in MCF7

cells is not BASP1-dependent as the fold changes in colony number and size observed in both shNEG and shBASP1 cells are similar. Therefore, the results suggest that EZH2 has an oncogenic role in MCF7 cells but BASP1 does not appear to be involved in this process.

The BASP1/WT1 complex is known to repress many genes involved in both cell growth and apoptosis[3]. Therefore, gene regulatory mechanisms are likely to be at play when EZH2 inhibition causes decreased cell growth in B-K562 cells and decreased tumorigenicity in shNEG MCF7 cells. In the presence of EZH2, BASP1 could potentially repress genes involved in apoptosis, like JUNB and c-MYC[84,85], by placing H3K27me3 marks. EZH2 was found to be recruited to WT1 target gene promoters in a BASP1-dependent manner[43]. However, coimmunoprecipitation experiments failed to demonstrate that BASP1 and EZH2 interact with each other. The BASP1 G2A mutant derivative, which is defective in transcriptional repression, was still able to mediate recruitment of EZH2 and lead to placement of H3K27me3. Thus, H3K27me3 is not sufficient to elicit transcriptional repression of WT1 target genes. Whether or not H3K27me3 is required for transcriptional repression by BASP1, or EZH2 is the enzyme responsible for its placement, is not clear. The EZH2 inhibitors were used to determine if this enzyme is required for transcriptional repression by BASP1.

4.2 BASP1 as a gene expression regulator

The four WT1 target genes analysed were AREG, JUNB, VDR and ETS-1. AREG, VDR and ETS-1 are involved in cell growth and development whereas JUNB is involved in cell apoptosis[84,86–88]. Treatment of K562 cells with UNC1999 resulted in significant increased JUNB expression in the treated B-K562 cells. In the absence of UNC1999, JUNB is normally repressed by BASP1 suggesting that BASP1 requires EZH2 to be able to repress JUNB. The increase in JUNB expression in treated B-K562 cells could potentially result in increased apoptosis which may explain why the treated B-K562 cells also have a decrease in cell growth. The same effect on JUNB is observed with inhibitors GSK343 and GSK126, however the increase in JUNB expression is not significant and more experiments are needed to confirm this.

AREG, which is a growth factor, remains significantly repressed in B-K562 cells treated with UNC1999 and GSK343. It also appears to remain repressed in B-

K562 cells treated with GSK126, but this was not found to be significant. AREG is a growth factor and thus its repression further correlates with the decrease in cell growth observed in treated K562 cells. These results also suggest that BASP1 has a different mechanism for repressing AREG and JUNB, since BASP1 can still repress AREG under conditions of EZH2 inhibition whereas it cannot repress JUNB. EZH2 is known to place H3K27me3 marks however, as mentioned in section 1.2.4, on WT1 target genes additional repressive H3K9me3 marks have also been found as well as BASP1-dependent removal of H3K9ac and H3K4me3 activatory marks[28,43]. Therefore, H3K27me3 marks alone do not repress AREG since by inhibiting EZH2, H3K27me3 marks are not placed and AREG is still repressed. ChIP analysis of H3K27me3 marks and H3K9ac marks on the promoter of AREG revealed that there is indeed a significant decrease in the levels of H3K27me3 in B-K562 cells treated with UNC1999 compared to treated V-K562 cells. This further confirms that EZH2 is responsible for placing H3K27me3 on AREG and that the placement of H3K27me3 marks is not required for transcriptional repression of AREG. The levels of H3K9ac marks do not change significantly between treated V-K562 and B-K562 cells as expected. More ChIP experiments would need to done analysing the levels of other activatory and repressive marks on AREG in order to determine the reasons that AREG remains repressed.

VDR and ETS-1 are both genes involved in development. They both appear to be affected by EZH2 inhibition in the same way. For both VDR and ETS-1, BASP1 caused robust transcriptional repression that was disrupted by the EZH2 inhibitors. This suggests that EZH2 enzymatic activity is required for BASP1 to repress these genes. These results differ from the results observed with AREG and JUNB suggesting that the mechanism of BASP1-mediated transcriptional repression depends on the target gene. ChIP analysis for VDR showed that there was no significant difference in the levels of H3K27me3 marks between V-K562 and B-K562 cells treated with UNC1999. There does however seem to be a decrease of H3K27me3 marks in both treated V-K562 and B-K562 cells compared to untreated V-K562 and B-K562 cells. This suggests that EZH2 can place H3K27me3 marks on VDR independently of BASP1 in both V-K562 and B-K562 cells. There is no significant difference in the levels of H3K9ac marks between treated V-K562 and B-K562 cells as expected.

Taken together, the results suggest that the BASP1/WT1 complex and EZH2 work together to repress target genes by placing H3K27me3 marks, however the mechanism is not the same for all genes. Figure 4.1 suggests two different mechanisms by which the BASP1/WT1 complex behaves, based on the results from the AREG and VDR genes (where both RNA and ChIP analysis was performed). At the AREG promoter BASP1 recruits EZH2 to methylate H3K27. When EZH2 is inhibited by UNC1999, methylation of H3K27 is reduced but the AREG gene is still repressed. At the VDR promoter the same EZH2 mechanism is at play, but the reduced H3K27 methylation in the presence of UNC1999 blocks BASP1-dependent repression of the gene. JUNB and ETS-1 likely function in a similar way to VDR, but ChIP analysis will be required to confirm this.

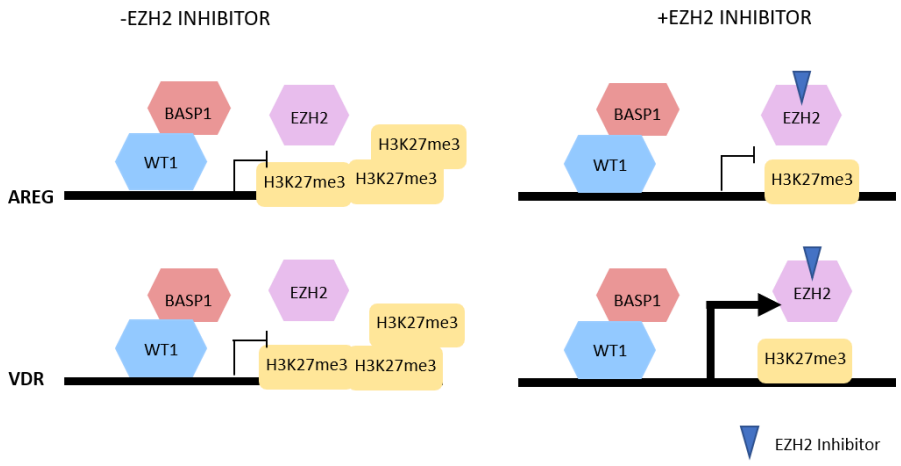

Figure 4.1: Proposed mechanism of BASP1/WT1-EZH2 mediated repression. The figure shows the promoter regions of the AREG and VDR genes. The BASP1/WT1 complex recruits EZH2 which places H3K27me3 marks resulting in gene repression. When EZH2 is inhibited by UNC1999 (indicated by the blue triangle), the levels of H3K27me3 are decreased. AREG is repressed in the presence of UNC1999 whereas VDR is expressed.

JUNB appears to be the gene most affected by EZH2 inhibition and this may be involved in the reduced growth rate of K562 cells. This could suggest a future therapeutic target of JUNB via EZH2 inhibition for CML patients. The results also suggest that the removal of the H3K27me3 marks from WT1 target gene promoters is not sufficient to reverse the repression from some of its target genes and so

further research into the other activatory and repressive marks found on the promoter regions of these genes could give further insight into the mechanism of BASP1/WT1 mediated transcriptional repression.

Despite the results suggesting that BASP1 and EZH2 work together, there has been no evidence provided so far showing that the two proteins interact, as mentioned previously. Therefore, the recruitment of PRC2 to the promoter of WT1 target genes, and therefore EZH2, could be dependent on a variety of other factors. The overall mechanism of PRC2 recruitment is not known but there have been many suggested mechanisms. One proposed mechanism suggests that the mono-ubiquitylation of lysine 199 on histone H2A (H2AK119ub1) by PRC1 leads to the recruitment of PRC2 by binding to the JARID2 subunit of the PRC2.2 complex[89]. Evidence has also been found that the PRC2 product, H3K27me3 marks, can also recruit PRC2[47]. EZH2 is activated by H3K27me3 binding to the core PRC2 subunit EED which leads to the 'spreading' of H3K27me3 marks and thus maintains the transcriptionally silent state of the gene. Studies have shown that RNA can be involved in the chromatin remodelling process and sometimes even have the ability to recruit chromatin remodelling factors[90]. The non-coding RNA (ncRNA) *HOTAIR* which is transcribed form the HOXC locus was found to drive the recruitment of PRC2 at the HOXD loci[91]. The HOX genes are involved in the development process, which BASP1 and WT1 are also involved in therefore this could be the mechanism of PRC2 recruitment of BASP1. Recent studies however have shown that *HOTAIR*-mediated repression can also occur independent of PRC2 and so the role of ncRNAs in PRC2 recruitment is not yet clear[92]. More recently, nascent RNA was found to bind to PRC2 and prevent PRC2 from interacting with the chromatin by acting as an antagonist[93]. This data corresponds with PRC2 being recruited to repressed genes to maintain their transcriptionally silent state.

Studies have also found that the presence of active chromatin marks, such as H3K4me3 which are found on WT1 target genes, can inhibit the recruitment of PRC2[94]. Therefore, the removal of active chromatin marks by the BASP1/WT1 complex through HDAC1 and Prohibitin could enable the recruitment of PRC2 to these genes. However, studies using the G2A-BASP1 which is not myristoylated and therefore cannot remove active chromatin marks from gene promoters showed that, EZH2 can still be recruited to the gene promoter region and place H3K27me3 marks.

Therefore, this proposed mechanism of PRC2 recruitment could not apply for WT1 target genes. As mentioned in section 1.2.5, the target genes of WT1 are bivalent so they can have both active and repressive chromatin marks found on the promoter region. This could explain why the AREG gene is being repressed even when the level of H3K27me3 marks decreases. The additional repressive marks found on the AREG promoter, such as H3K9me3, could be sufficient to repress AREG. The removal of active chromatin marks by BASP1 could also be sufficient to repress AREG. Further experiments with the G2A-BASP1 could show why the H3K27me3 marks are not enough to repress AREG. Further research into BASP1-dependent chromatin marks could also provide a novel mechanism by which PRC2 is recruited by BASP1.

5.Further Experiments

5.1 Validating the role of EZH2 in the BASP1/WT1 complex

ChIP experiments in this study were only performed on the AREG and VDR genes using the UNC1999 inhibitor. Therefore, ChIP experiments also need to be performed on the JUNB and ETS-1 genes and with the GSK343 and GSK126 inhibitors to establish if the same pattern is seen with all three inhibitors. Gene expression analysis and ChIP experiments should also be carried out in MCF7 cells using the same genes and inhibitors to determine if the same effect occurs in a different cell line. To validate the results found using the EZH2 inhibitors, siRNA targeting EZH2 can be used to ensure that the specific inhibition of EZH2 is the cause for the results observed. CRISPR-Cas9-mediated knockout of EZH2 can also be used however, recent studies showed that CRISPR-Cas9 EZH2 knockout results in decreased cell viability in neuroblastoma cells[95].

5.2 The role of PRC2 in the BASP1/WT1 complex

Inhibition of other PRC2 core subunits such as EED, SUZ12 and RBBP46/48 followed by WT1 target gene expression analysis and ChIP should also be done to establish if the whole PRC2 complex is involved in BASP1/WT1 mediated repression. Analysis of other chromatin marks found on WT1 target gene promoters, like H3K9me3 and H3K4me3, should be performed using ChIP experiments to show how the levels of other activatory or repressive marks change when the genes are repressed by BASP1. The mechanism by which PRC2 is recruited by BASP1 can be studied by targeting active histone marks known to inhibit PRC2 recruitment.

5.3 The role of chromatin remodelling factors in the BASP1/WT1 complex

Previous Mass Spectrometry experiments by our lab showing BASP1-binding proteins identified several chromatin remodelling proteins such as KDM4B and NSD3[43]. KMD4B (also known as JMJD2B) is a histone demethylase protein shown to be involved in the removal of methyl groups from H3K9, one of the repressive marks found on WT1 target genes[96]. NSD3 is a histone methyltransferase found to be involved in the methylation of H3K27 and H3K4, repressive and activatory marks respectively found on WT1 target genes[97]. ChIP experiments can therefore be carried out to study if these proteins are being recruited by BASP1 like EZH2. If these proteins are being recruited by BASP1, further experiments using siRNA and inhibitors

targeting these proteins can be carried out in a similar way to the experiments carried out in this study for EZH2.

5.4 Role of EZH2 in podocyte development

Conditional knockout studies of WT1 in podocyte cells have shown that loss of WT1 results in the loss of foot processes in the podocyte cells which leads to death caused by severe kidney failure[98]. This showed that WT1 expression is essential in the kidney of the adult mouse. Conditional knockout studies of EZH2 in podocyte cells could show if EZH2 is necessary for normal kidney function. Such findings would be consistent with a role for EZ~~H~~2 in BASP1/WT1 function in podocyte cells. Follow-up experiments to demonstrate a functional interaction, such as ChIP and RNA analysis, would provide evidence that EZH2 is involved in BASP1/WT1-mediated transcriptional regulation.

6.Appendix

6.1 Melt Curves for RNA analysis

When samples were analysed on a qPCR machine to study the levels of gene expression, melt curves were also made as explained in section 2.8. the melt curves indicated a single peak were the double-stranded DNA primer would break and the fluorescence from SYBR green could be measured. The melt curved validated that the samples were not contaminated by any non-specific DNA products. The melt curves are shown in Figures 6.1, 6.2 and 6.3.

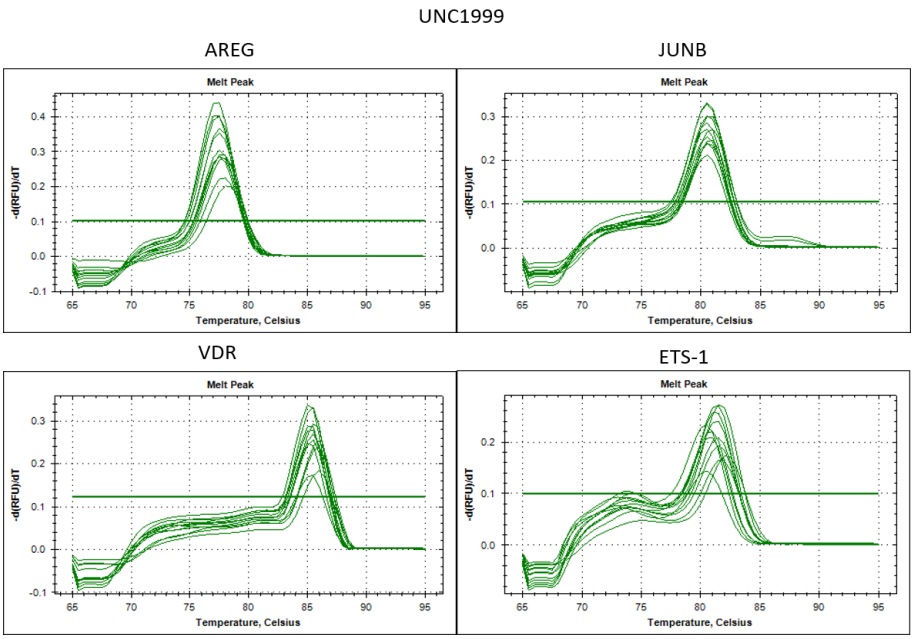

Figure 6.1: Melt curves for RNA analysis of K562 cells with UNC1999. Melt curve analysis of the AREG, JUNB, VDR and ETS-1 genes following 72h treatment with UNC1999 in K562 cells. Peak indicates the temperature in °Celsius at which the double-stranded DNA of each gene primer breaks.

GSK343

AREG

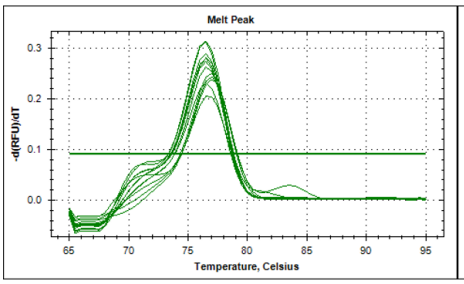

JUNB

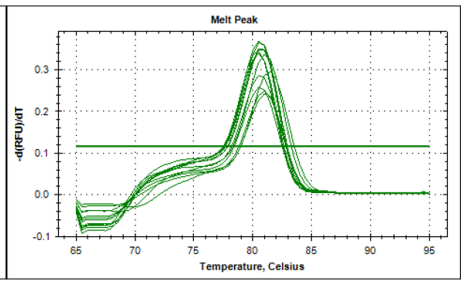

VDR

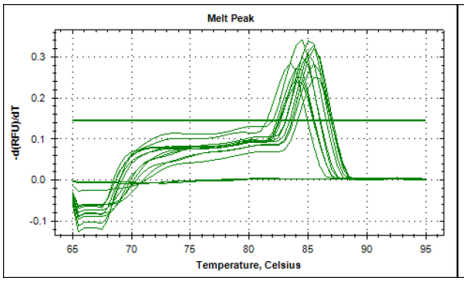

ETS-1

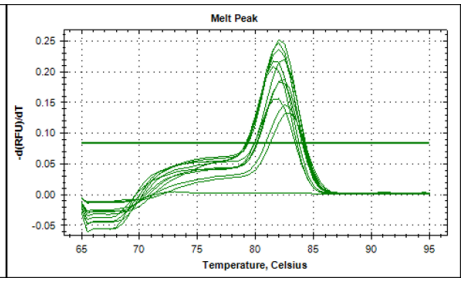

<u>Figure 6.2:</u> Melt curves for RNA analysis of K562 cells with GSK343. Melt curve analysis of the AREG, JUNB, VDR and ETS-1 genes following 72h treatment with GSK343 in K562 cells. Peak indicates the temperature in °Celsius at which the double-stranded DNA of each gene primer breaks.

GSK126

AREG

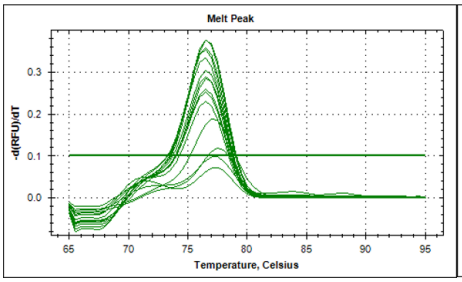

JUNB

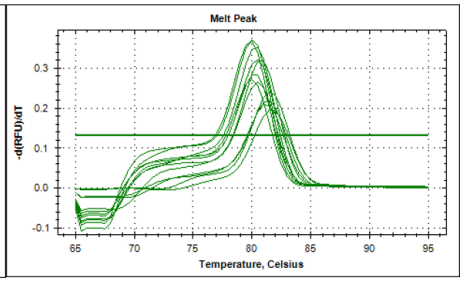

VDR

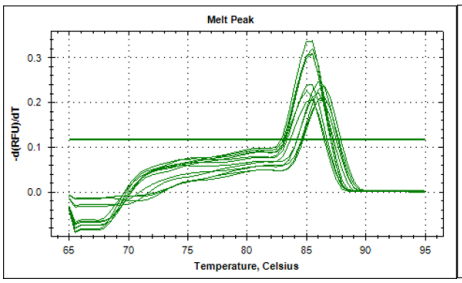

ETS-1

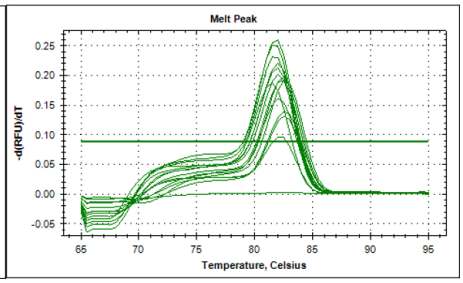

Figure 6.3: Melt curves for RNA analysis of K562 cells with GSK126. Melt curve analysis of the AREG, JUNB, VDR and ETS-1 genes following 72h treatment with GSK126 in K562 cells. Peak indicates the temperature in °Celsius at which the double-stranded DNA of each gene primer breaks.

6.2 DNA gel for sonication analysis

A DNA gel was run after cells were sonicated for ChIP experiments as explained in section 2.9. this was done to validate that the DNA in the cells was successfully sheared to produce small DNA fragments between 200 and 500 base pairs. The DNA gel is shown in Figure 6.4.

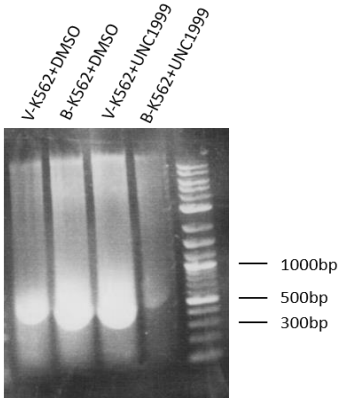

Figure 6.4: DNA gel showing successful sonication of K562 cells. Gel electrophoresis following K562 cell sonication to show the size of DNA fragments. Base pair markers (bp) are shown on the right.

6.3 Melt Curves for ChIP analysis

Melt curves made in the same way as explained in section 6.1. Melt curves for ChIP analysis of K562 cells following treatment with UNC1999 shown in Figure 6.5.

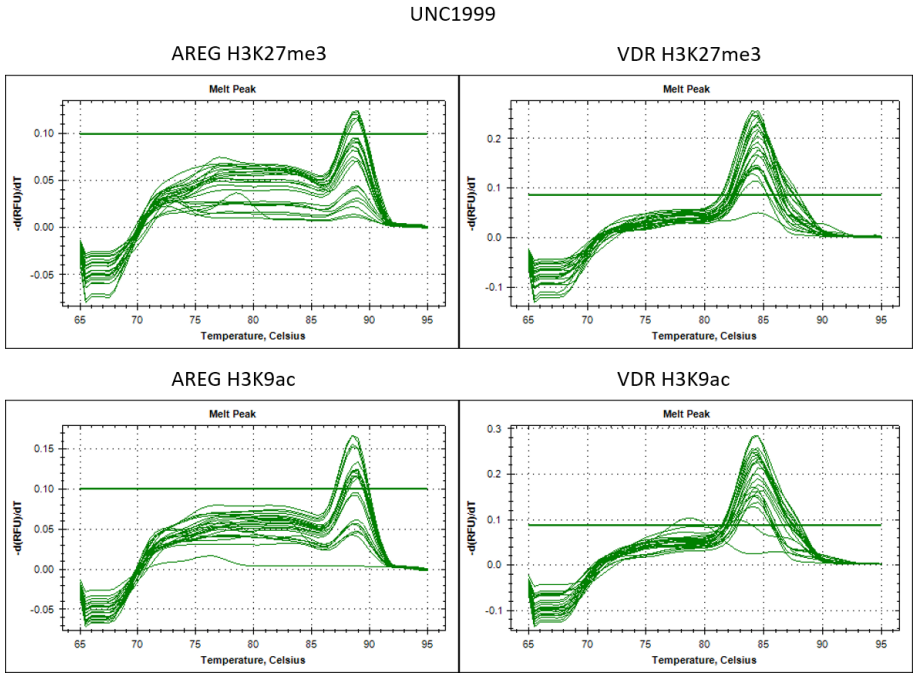

Figure 6.5: Melt curves for ChIP analysis of K562 cells with UNC1999. Melt curve analysis of the AREG and VDR genes following 48h treatment with UNC1999 in K562 cells. Peak indicates the temperature in °Celsius at which the double-stranded DNA of each gene primer breaks.

7.References

1. Szychot, E., Apps, J. & Pritchard-Jones, K. et al. Wilms' tumor: biology, diagnosis and treatment. *Transl. Pediatr.* (2014). doi:10.3978/j.issn.2224-4336.2014.01.09

2. Hastie, N. D. *THE GENETICS OF WILMS' TUMOR-A Case of Disrupted Development*. (1994).

3. Toska, E. & Roberts, S. G. E. Mechanisms of transcriptional regulation by WT1 (Wilms' tumour 1). *Biochem. J.* **461**, 15–32 (2014).

4. Roberts, S. G. E. In vitro transcription to study WT1 function. in *Methods in Molecular Biology* (2016). doi:10.1007/978-1-4939-4023-3_13

5. Haber, D. A. *et al.* An internal deletion within an 11p13 zinc finger gene contributes to the development of Wilms' tumor. *Cell* (1990). doi:10.1016/0092-8674(90)90690-G

6. Haber, D. A. *et al.* Alternative splicing and genomic structure of the Wilms tumor gene WT1. *Proc. Natl. Acad. Sci.* **88**, 9618–9622 (1991).

7. Wang, Z.-Y., Qiu, Q.-Q., Enger, K. T. & Deuel, T. F. *A second transcriptionally active DNA-binding site for the Wilms tumor gene product, WT1 (zinc-finger protein/suppressor/gene regulation)*. *Proc. Natl. Acad. Sci. USA* **90**, (1993).

8. Mrowka, C. & Schedl, A. *Wilms' Tumor Suppressor Gene WT1: From Structure to Renal Pathophysiologic Features*. (2000).

9. Ullmark, T., Montano, G. & Gullberg, U. DNA and RNA binding by the Wilms' tumour gene 1 (WT1) protein +KTS and −KTS isoforms—From initial observations to recent global genomic analyses. *European Journal of Haematology* (2018). doi:10.1111/ejh.13010

10. Green, L. M., Wagner, K. J., Campbell, H. A., Addison, K. & Roberts, S. G. E. Dynamic interaction between WT1 and BASP1 in transcriptional regulation during differentiation. *Nucleic Acids Res.* **37**, 431–40 (2009).

11. Miles, C. G. *et al.* Mice Lacking the 68-Amino-Acid, Mammal-Specific N-Terminal Extension of WT1 Develop Normally and Are Fertile. *Mol. Cell. Biol.* (2003). doi:10.1128/mcb.23.7.2608-2613.2003

12. Smolen, G. A., Vassileva, M. T., Wells, J., Matunis, M. J. & Haber, D. A. SUMO-1 modification of the Wilms' tumor suppressor WT1. *Cancer Res.* (2004). doi:10.1158/0008-5472.CAN-04-1502

13. Sakamoto, Y., Yoshida, M., Semba, K. & Hunter, T. *Inhibition of the DNA-binding and transcriptional repression activity of the Wilms' tumor gene product, WT1, by cAMP-dependent protein kinase-mediated phosphorylation of Ser-365 and Ser-393 in the zinc ®nger domain*. (1997).

14. Ye, Y., Raychaudhuri, B., Gurney, A., Campbell, C. E. & Williams, B. R. Regulation of WT1 by phosphorylation: inhibition of DNA binding, alteration of transcriptional activity and cellular translocation. *EMBO J.* (1996).

15. Wang, W., Lee, S. B., Palmer, R., Ellisen, L. W. & Haber, D. A. A Functional Interaction with CBP Contributes to Transcriptional Activation by the Wilms Tumor Suppressor WT1. *J. Biol. Chem.* (2001). doi:10.1074/jbc.M009687200

16. Carpenter, B. *et al.* BASP1 is a transcriptional cosuppressor for the Wilms' tumor suppressor

protein WT1. *Mol. Cell. Biol.* (2004). doi:10.1128/mcb.24.2.537-549.2004

17. Maheswaran, S. *et al.* Physical and functional interaction between WT1 and p53 proteins. *Proc. Natl. Acad. Sci.* (2006). doi:10.1073/pnas.90.11.5100

18. Kreidberg, J. A. *et al.* WT-1 is required for early kidney development. *Cell* (1993). doi:10.1016/0092-8674(93)90515-R

19. Pelletier, J. *et al.* Germline mutations in the Wilms' tumor suppressor gene are associated with abnormal urogenital development in denys-drash syndrome. *Cell* (1991). doi:10.1016/0092-8674(91)90194-4

20. Rose, E. A. *et al.* Complete physical map of the WAGR region of 11p13 localizes a candidate Wilms' tumor gene. *Cell* (1990). doi:10.1016/0092-8674(90)90600-J

21. Koesters, R. *et al.* WT1 is a tumor-associated antigen in colon cancer that can be recognized by in vitro stimulated cytotoxic T cells. *Int. J. cancer* **109**, 385–92 (2004).

22. Artibani, M. *et al.* WT1 expression in breast cancer disrupts the epithelial/mesenchymal balance of tumour cells and correlates with the metabolic response to docetaxel. *Sci. Rep.* (2017). doi:10.1038/srep45255

23. Loeb, D. M. *et al.* Wilms' Tumor Suppressor Gene (WT1) Is Expressed in Primary Breast Tumors Despite Tumor-specific Promoter Methylation. *Cancer Res.* **61**, (2001).

24. Oji, Y. *et al.* Overexpression of the Wilms' tumor gene W T1 in primary astrocytic tumors. *Cancer Sci.* **95**, 822–7 (2004).

25. Goodfellow, S. J. *et al.* WT1 and its transcriptional cofactor BASP1 redirect the differentiation pathway of an established blood cell line. *Biochem. J.* (2011). doi:10.1042/bj20101734

26. Mosevitsky, M. I. *et al.* The BASP1 family of myristoylated proteins abundant in axonal termini. Primary structure analysis and physico-chemical properties. *Biochimie* **79**, 373–84 (1997).

27. Hartl, M. & Schneider, R. A Unique Family of Neuronal Signaling Proteins Implicated in Oncogenesis and Tumor Suppression. *Front. Oncol.* (2019). doi:10.3389/fonc.2019.00289

28. Toska, E. *et al.* Repression of Transcription by WT1-BASP1 Requires the Myristoylation of BASP1 and the PIP2-Dependent Recruitment of Histone Deacetylase. *Cell Rep.* (2012). doi:10.1016/j.celrep.2012.08.005

29. Epand, R. F., Sayer, B. G. & Epand, R. M. Induction of raft-like domains by a myristoylated NAP-22 peptide and its Tyr mutant. *FEBS J.* **272**, 1792–803 (2005).

30. Rechsteiner, M. & Rogers, S. W. PEST sequences and regulation by proteolysis. *Trends in Biochemical Sciences* (1996). doi:10.1016/S0968-0004(96)10031-1

31. Guo, R.-S. *et al.* Restoration of Brain Acid Soluble Protein 1 Inhibits Proliferation and Migration of Thyroid Cancer Cells. *Chin. Med. J. (Engl).* **129**, 1439–46 (2016).

32. Moribe, T. *et al.* Identification of novel aberrant methylation of BASP1 and SRD5A2 for early diagnosis of hepatocellular carcinoma by genome-wide search. *Int. J. Oncol.* **33**, 949–58 (2008).

33. Marsh, L. A. *et al.* BASP1 interacts with oestrogen receptor α and modifies the tamoxifen response. *Cell Death Dis.* (2017). doi:10.1038/cddis.2017.179

34. Tang, H. *et al.* High brain acid soluble protein 1(BASP1) is a poor prognostic factor for cervical

cancer and promotes tumor growth. *Cancer Cell Int.* **17**, 97 (2017).

35. Gao, Y., Dutta Banik, D., Muna, M. M., Roberts, S. G. & Medler, K. F. The WT1–BASP1 complex is required to maintain the differentiated state of taste receptor cells. *Life Sci. Alliance* (2019). doi:10.26508/lsa.201800287

36. Gao, Y., Toska, E., Denmon, D., Roberts, S. G. E. & Medler, K. F. WT1 regulates the development of the posterior taste field. *Dev.* **141**, 2271–2278 (2014).

37. Barlow, L. A. & Klein, O. D. Developing and regenerating a sense of taste. in *Current Topics in Developmental Biology* **111**, 401–419 (Academic Press Inc., 2015).

38. Blanchard, J. W. *et al.* Replacing reprogramming factors with antibodies selected from combinatorial antibody libraries. *Nat. Biotechnol.* (2017). doi:10.1038/nbt.3963

39. Boland, M. J. *et al.* Adult mice generated from induced pluripotent stem cells. *Nature* **461**, 91–94 (2009).

40. Cho, J. *et al.* LIN28A is a suppressor of ER-associated translation in embryonic stem cells. *Cell* **151**, 765–777 (2012).

41. Toska, E., Shandilya, J., Goodfellow, S. J., Medler, K. F. & Roberts, S. G. E. Prohibitin is required for transcriptional repression by the WT1-BASP1 complex. *Oncogene* (2013). doi:10.1038/onc.2013.447

42. Trotter, K. W. & Archer, T. K. The BRG1 transcriptional coregulator. *Nucl. Recept. Signal.* (2008). doi:10.1621/nrs.06004

43. Dey, A. E. Investigating the Role of BASP1 Lipidation in WT1/BASP1 Mediated Repression. (University of Bristol, 2019).

44. Essafi, A. *et al.* A wt1-controlled chromatin switching mechanism underpins tissue-specific wnt4 activation and repression. *Dev. Cell* **21**, 559–74 (2011).

45. Martínez-Estrada, O. M. *et al.* Wt1 is required for cardiovascular progenitor cell formation through transcriptional control of Snail and E-cadherin. *Nat. Genet.* (2010). doi:10.1038/ng.494

46. Bernstein, B. E. *et al.* A bivalent chromatin structure marks key developmental genes in embryonic stem cells. *Cell* (2006). doi:10.1016/j.cell.2006.02.041

47. Hansen, K. H. *et al.* A model for transmission of the H3K27me3 epigenetic mark. *Nat. Cell Biol.* (2008). doi:10.1038/ncb1787

48. Gö Tz Laible, G. *et al. Mammalian homologues of the Polycomb-group gene Enhancer of zeste mediate gene silencing in Drosophila heterochromatin and at S.cerevisiae telomeres of expression boundaries within the homeotic gene cluster*. *The EMBO Journal* **16**, (Simon, 1997).

49. Schuettengruber, B., Bourbon, H. M., Di Croce, L. & Cavalli, G. Genome Regulation by Polycomb and Trithorax: 70 Years and Counting. *Cell* **171**, 34–57 (2017).

50. Lee, T. I. *et al.* Control of Developmental Regulators by Polycomb in Human Embryonic Stem Cells. *Cell* **125**, 301–313 (2006).

51. Ezhkova, E. *et al.* Ezh2 Orchestrates Gene Expression for the Stepwise Differentiation of Tissue-Specific Stem Cells. *Cell* **136**, 1122–1135 (2009).

52. Kuzmichev, A., Nishioka, K., Erdjument-Bromage, H., Tempst, P. & Reinberg, D. Histone methyltransferase activity associated with a human multiprotein complex containing the

enhancer of zeste protein. *Genes Dev.* **16**, 2893–2905 (2002).

53. Visser, H. P. J. *et al.* The Polycomb group protein EZH2 is upregulated in proliferating, cultured human mantle cell lymphoma. *Br. J. Haematol.* **112**, 950–958 (2001).

54. Margueron, R. *et al.* Ezh1 and Ezh2 Maintain Repressive Chromatin through Different Mechanisms. *Mol. Cell* **32**, 503–518 (2008).

55. Son, J., Shen, S. S., Margueron, R. & Reinberg, D. Nucleosome-binding activities within JARID2 and EZH1 regulate the function of PRC2 on chromatin. *Genes Dev.* **27**, 2663–2677 (2013).

56. Margueron, R. & Reinberg, D. The Polycomb complex PRC2 and its mark in life. *Nature* **469**, 343–349 (2011).

57. Whitcomb, S. J., Basu, A., Allis, C. D. & Bernstein, E. Polycomb Group proteins: an evolutionary perspective. *Trends Genet.* **23**, 494–502 (2007).

58. Hauri, S. *et al.* A High-Density Map for Navigating the Human Polycomb Complexome. *Cell Rep.* **17**, 583–595 (2016).

59. Cao, R. *et al.* Role of histone H3 lysine 27 methylation in polycomb-group silencing. *Science (80-.).* **298**, 1039–1043 (2002).

60. Brien, G. L. *et al.* Polycomb PHF19 binds H3K36me3 and recruits PRC2 and demethylase NO66 to embryonic stem cell genes during differentiation. *Nat. Struct. Mol. Biol.* **19**, 1273–1281 (2012).

61. Grijzenhout, A. *et al.* Functional analysis of AEBP2, a PRC2 Polycomb protein, reveals a Trithorax phenotype in embryonic development and in ESCs. *Development* **143**, 2716–2723 (2016).

62. Li, H. *et al.* Polycomb-like proteins link the PRC2 complex to CpG islands. *Nature* **549**, 287–291 (2017).

63. Pasini, D. *et al.* JARID2 regulates binding of the Polycomb repressive complex 2 to target genes in ES cells. *Nature* **464**, 306–310 (2010).

64. Wang, H. *et al.* Role of histone H2A ubiquitination in Polycomb silencing. *Nature* **431**, 873–878 (2004).

65. Bracken, A. P., Dietrich, N., Pasini, D., Hansen, K. H. & Helin, K. Genome-wide mapping of polycomb target genes unravels their roles in cell fate transitions. *Genes Dev.* **20**, 1123–1136 (2006).

66. Laugesen, A., Højfeldt, J. W. & Helin, K. Molecular Mechanisms Directing PRC2 Recruitment and H3K27 Methylation. *Mol. Cell* **74**, 8–18 (2019).

67. Kim, K. H. & Roberts, C. W. M. Targeting EZH2 in cancer. *Nature Medicine* **22**, 128–134 (2016).

68. Varambally, S. *et al.* The polycomb group protein EZH2 is involved in progression of prostate cancer. *Nature* **419**, 624–629 (2002).

69. Bachmann, I. M. *et al.* EZH2 expression is associated with high proliferation rate and aggressive tumor subgroups in cutaneous melanoma and cancers of the endometrium, prostate, and breast. *J. Clin. Oncol.* **24**, 268–273 (2006).

70. Bracken, A. P. *et al.* EZH2 is downstream of the pRB-E2F pathway, essential for proliferation and amplified in cancer. *EMBO J.* **22**, 5323–5335 (2003).

71. Bödör, C. *et al.* EZH2 Y641 mutations in follicular lymphoma. *Leukemia* **25**, 726–729 (2011).

72. Yap, D. B. *et al.* Somatic mutations at EZH2 Y641 act dominantly through a mechanism of selectively altered PRC2 catalytic activity, to increase H3K27 trimethylation. *Blood* **117**, 2451–2459 (2011).

73. Majer, C. R. *et al.* A687V EZH2 is a gain-of-function mutation found in lymphoma patients. *FEBS Lett.* **586**, 3448–3451 (2012).

74. McCabe, M. T. *et al.* Mutation of A677 in histone methyltransferase EZH2 in human B-cell lymphoma promotes hypertrimethylation of histone H3 on lysine 27 (H3K27). *Proc. Natl. Acad. Sci. U. S. A.* **109**, 2989–2994 (2012).

75. Chang, C. J. *et al.* EZH2 promotes expansion of breast tumor initiating cells through activation of RAF1-β-catenin signaling. *Cancer Cell* **19**, 86–100 (2011).

76. Kadoch, C. *et al.* Proteomic and bioinformatic analysis of mammalian SWI/SNF complexes identifies extensive roles in human malignancy. *Nat. Genet.* **45**, 592–601 (2013).

77. Wilson, B. G. *et al.* Epigenetic antagonism between polycomb and SWI/SNF complexes during oncogenic transformation. *Cancer Cell* **18**, 316–328 (2010).

78. Ernst, T. *et al.* Inactivating mutations of the histone methyltransferase gene EZH2 in myeloid disorders. *Nat. Genet.* **42**, 722–726 (2010).

79. Simon, C. *et al.* A key role for EZH2 and associated genes in mouse and human adult T-cell acute leukemia. *Genes Dev.* **26**, 651–656 (2012).

80. Lue, J. K. & Amengual, J. E. Emerging EZH2 Inhibitors and Their Application in Lymphoma. *Curr. Hematol. Malig. Rep.* **13**, 369–382 (2018).

81. Verma, S. K. *et al.* Identification of potent, selective, cell-Active inhibitors of the histone lysine methyltransferase EZH2. *ACS Med. Chem. Lett.* **3**, 1091–1096 (2012).

82. McCabe, M. T. *et al.* EZH2 inhibition as a therapeutic strategy for lymphoma with EZH2-activating mutations. *Nature* **492**, 108–112 (2012).

83. Konze, K. D. *et al.* An orally bioavailable chemical probe of the lysine methyltransferases EZH2 and EZH1. *ACS Chem. Biol.* **8**, 1324–1334 (2013).

84. Kim, H. S. *et al.* Identification of novel Wilms' tumor suppressor gene target genes implicated in kidney development. *J. Biol. Chem.* **282**, 16278–16287 (2007).

85. Zhang, X., Xing, G. & Saunders, G. F. Proto-oncogene N-myc promoter is down regulated by the Wilms' tumor suppressor gene WT1. *Anticancer Res.* **19**, 1641–8

86. Lee, S. B. *et al.* The Wilms tumor suppressor WT1 encodes a transcriptional activator of amphiregulin. *Cell* **98**, 663–673 (1999).

87. LEE, T. H. & PELLETIER, J. Functional characterization of WT1 binding sites within the human vitamin D receptor gene promoter. *Physiol. Genomics* **7**, 187–200 (2001).

88. Wagner, N., Michiels, J. F., Schedl, A. & Wagner, K. D. The Wilms' tumour suppressor WT1 is involved in endothelial cell proliferation and migration: Expression in tumour vessels in vivo. *Oncogene* **27**, 3662–3672 (2008).

89. Blackledge, N. P. *et al.* Variant PRC1 complex-dependent H2A ubiquitylation drives PRC2 recruitment and polycomb domain formation. *Cell* **157**, 1445–1459 (2014).

90. Bernstein, E. & Allis, C. D. RNA meets chromatin. *Genes and Development* **19**, 1635–1655 (2005).

91. Rinn, J. L. *et al.* Functional Demarcation of Active and Silent Chromatin Domains in Human HOX Loci by Noncoding RNAs. *Cell* **129**, 1311–1323 (2007).

92. Portoso, M. *et al.* PRC 2 is dispensable for HOTAIR -mediated transcriptional repression . *EMBO J.* **36**, 981–994 (2017).

93. Beltran, M. *et al.* The interaction of PRC2 with RNA or chromatin s mutually antagonistic. *Genome Res.* **26**, 896–907 (2016).

94. Schmitges, F. W. *et al.* Histone Methylation by PRC2 Is Inhibited by Active Chromatin Marks. *Mol. Cell* **42**, 330–341 (2011).

95. Chen, L. *et al.* CRISPR-Cas9 screen reveals a MYCN-amplified neuroblastoma dependency on EZH2. *J. Clin. Invest.* **128**, 446–462 (2018).

96. Cloos, P. A. C. *et al.* The putative oncogene GASC1 demethylates tri- and dimethylated lysine 9 on histone H3. *Nature* **442**, 307–311 (2006).

97. Morishita, M., Mevius, D. & Di Luccio, E. In vitro histone lysine methylation by NSD1, NSD2/MMSET/WHSC1 and NSD3/WHSC1L. *BMC Struct. Biol.* **14**, (2014).

98. Chau, Y. Y. *et al.* Acute multiple organ failure in adult mice deleted for the developmental regulator Wt1. *PLoS Genet.* **7**, (2011).